Global Navigation Satellite Systems
and
Ionospheric Remote Sensing

Jade Morton

Miami University

Our Increasing Dependence on GNSS Services, ….

Global Navigation Satellite Systems & Ionosphere

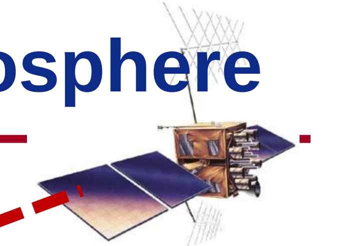

Ionosphere:
Dynamic
Difficult to model
Introduces error, disruptive

GNSS:
Passive
Well defined signals
Global coverage, distributed

Ionosphere

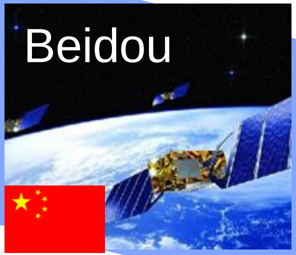

By 2023:
>160 GNSS satellites
>400 signals

1. **Ionosphere** impact **GNSS** performances
2. **GNSS** offers an excellent means to study **ionosphere**

Presentation Outline

1. **Ionosphere background**
2. **First order ionosphere error and TEC**
3. **Higher order ionosphere error**
4. **Ionosphere scintillation**

Ionosphere Background

$$\rho = v\Delta t$$

$$v = c / n$$

n: Reflective index
c: Speed of light

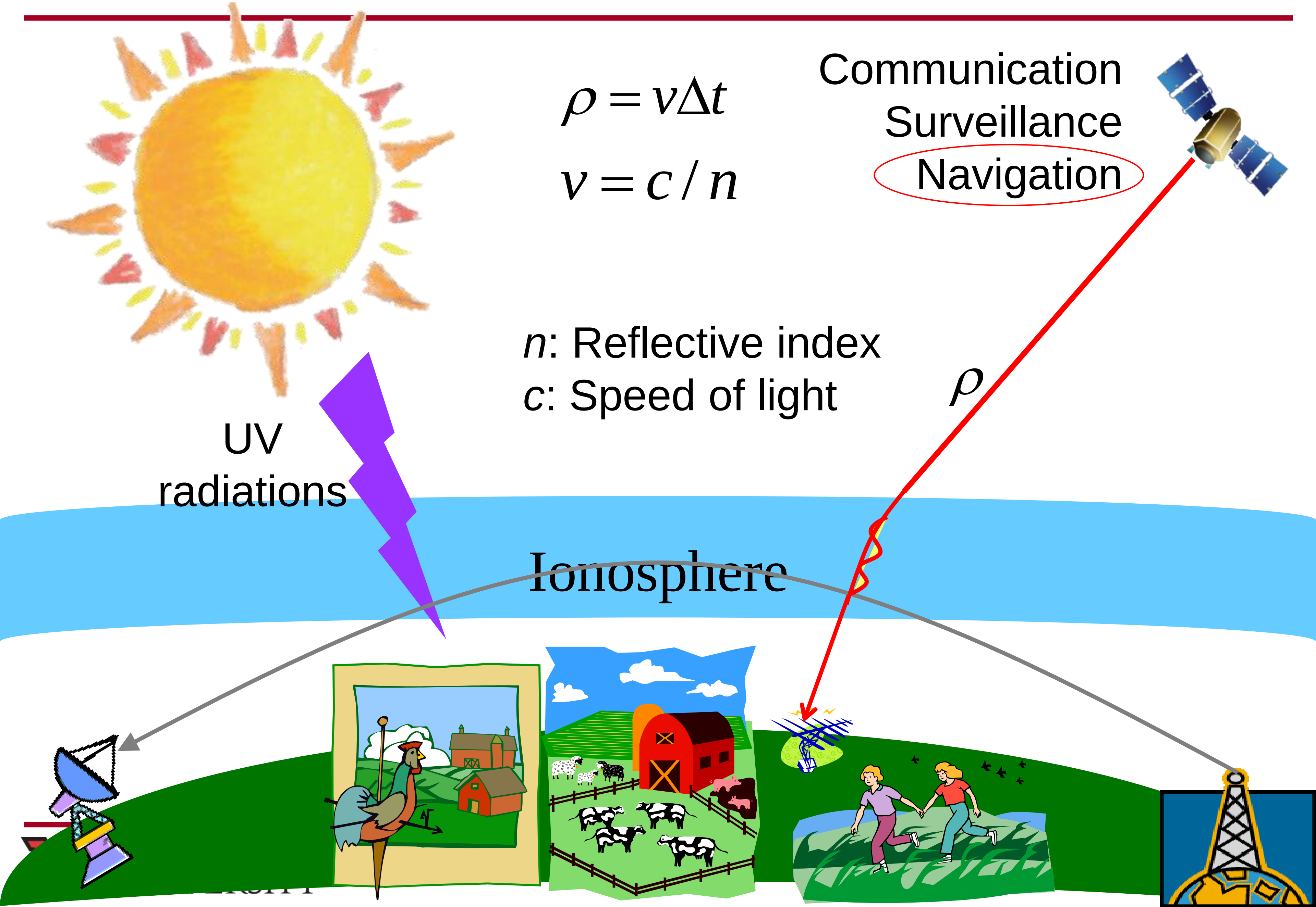

Ionosphere Refractive Index

Appleton-Hartree Equation:

$$n_\phi = 1 - \frac{X}{1 - \frac{Y^2 \sin^2\theta_B}{2(1-X)} \pm \sqrt{\frac{Y^4 \sin^4\theta_B}{4(1-X)^2} + Y^2\cos^2\theta_B}}$$

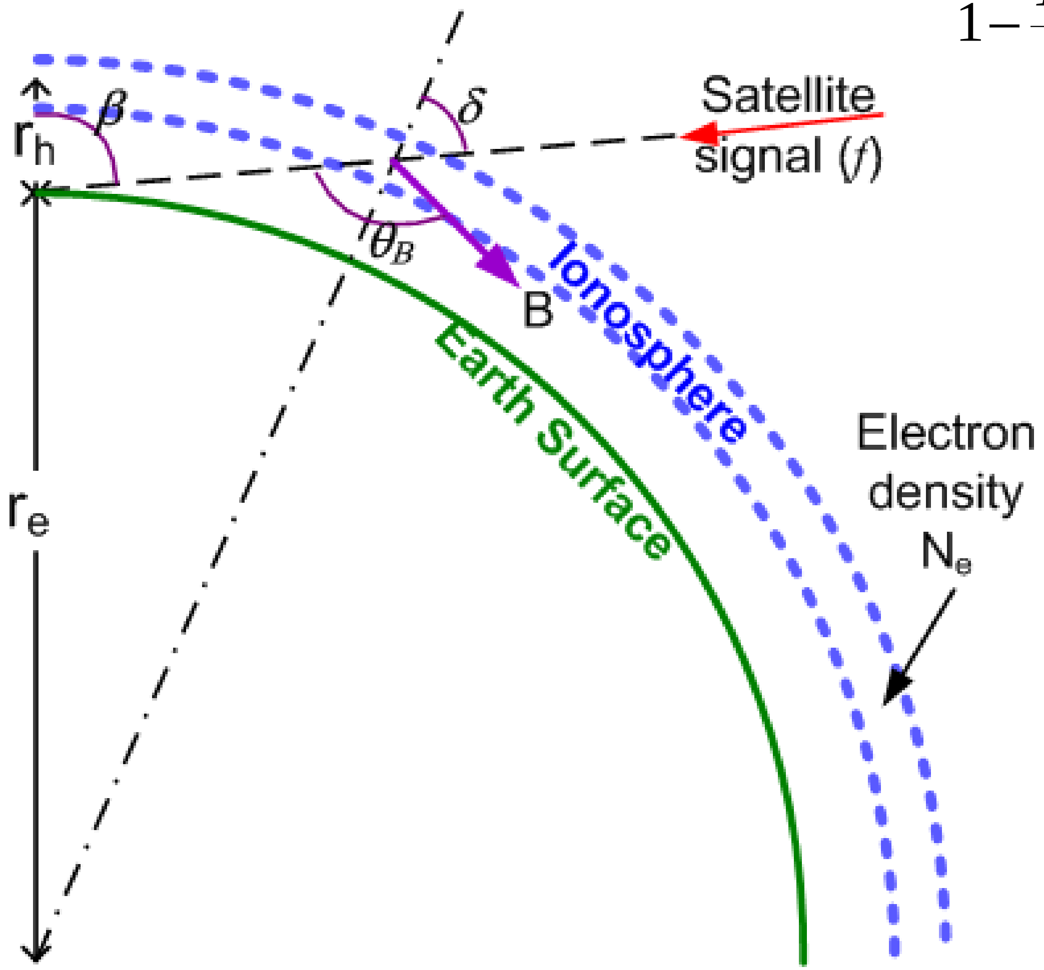

$$X = \left(\frac{f_p}{f}\right)^2 \qquad Y = \frac{f_g}{f}$$

Electron gyro frequency $f_g = \frac{|e|B}{m_e}$

Plasma frequency $f_p = \sqrt{\frac{N_e e^2}{m_e \varepsilon_0}}$

Electron Gryo Frequency

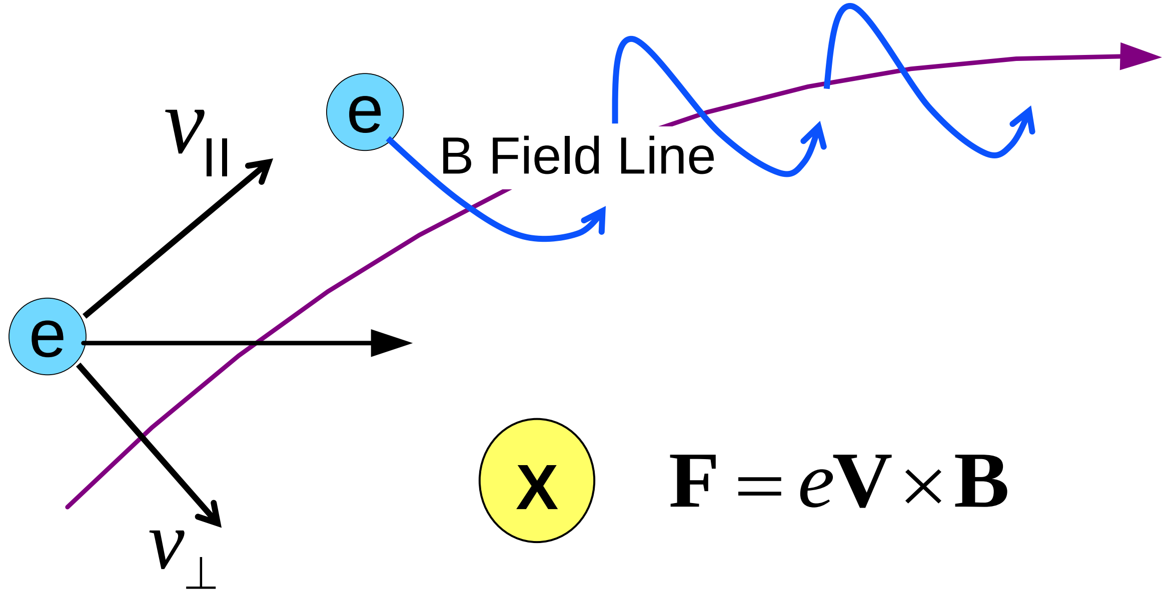

$$\mathbf{F} = e\mathbf{V} \times \mathbf{B}$$

f_g: Rate of electrons cycling along the **B** field line

$$f_g = \frac{|e|B}{2\pi m_e} \approx 28 \times 10^9 B \approx 1MHz$$

$$\downarrow$$

30,000nT ~ 3x10^{-5} T

Plasma Frequency

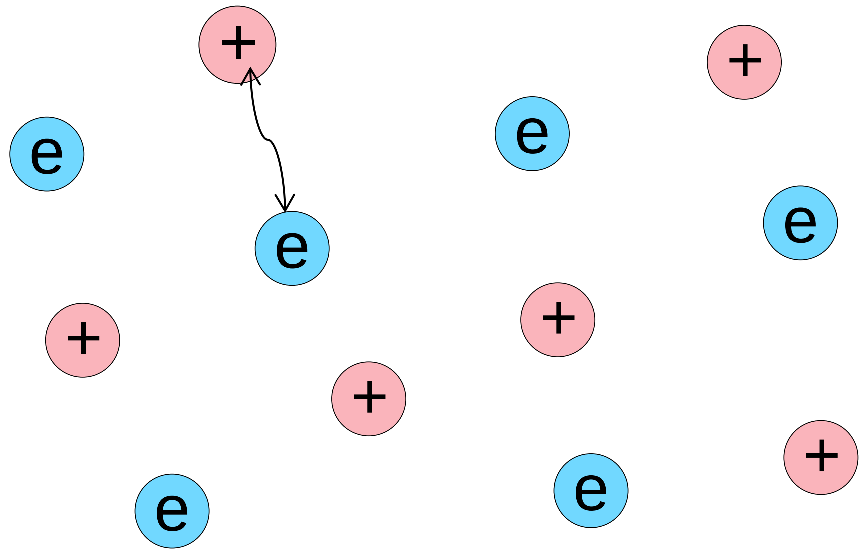

f_p: Rate of electron oscillations in a plasma

$$f_p = \frac{1}{2\pi}\sqrt{\frac{N_e e^2}{m_e \varepsilon_0}} \approx 9\sqrt{N_e} \approx 9MHz$$

Peak ionosphere N_e value: 1 million/cc

Simplified Appleton-Hartree Equation

$$f_g \approx 1MHz \longrightarrow Y = \frac{f_g}{f} \qquad f_p \le 10MHz \longrightarrow X = \left(\frac{f_p}{f}\right)^2$$

At GPS frequency, f ~ GHz: $X << 1 \qquad Y << 1$

$$n_\phi = 1 - \frac{X}{1 - \frac{Y^2 \sin^2\theta_B}{2(1-X)} \pm \sqrt{\frac{Y^4 \sin^4\theta_B}{4(1-X)^2} + Y^2\cos^2\theta_B}}$$

$$\underbrace{n_\phi \approx 1}_{\text{Vacuum}} \underbrace{- \frac{X}{2}}_{1^{st}\text{ order}} \underbrace{\pm XY|\cos\theta_B|}_{2^{nd}\text{ order}} \underbrace{- \frac{1}{4}X\left(\frac{X}{2} + Y^2(1+\cos^2\theta_B)\right)}_{3^{rd}\text{ order}}$$

Ionosphere Error in GNSS Measurements

$$n_\phi \approx 1 - \frac{40.3 N_e}{f^2} \pm \frac{f_g f_p^2}{2 f^3} \left| \cos\theta_B \right| - \ldots \qquad n_\rho = n_\phi + f \frac{dn_\phi}{df}$$

$$I_\phi = \int (n_\phi - 1) dl \qquad I_\rho = \int (n_\rho - 1) dl$$

$$I_\rho = \frac{q}{f^2} + \frac{s}{f^3} + \frac{r}{f^4} + \cdots \qquad I_\phi = -\frac{q}{f^2} - \frac{s}{2 f^3} - \frac{r}{3 f^4} + \cdots$$

First order ionosphere error: $q = 40.3 \times \int N_e dl = 40.3 TEC$

Second order ionosphere error: $s = 7527 c \int N_e B_0 \cos\theta_B dl$

3rd order: $r = 2437 \int N_e^2 dl + 4738 \times 10^{22} \int N_e B_0^2 \left(2 + \cos^2\theta_B\right) dl$

First Order Ionosphere Error

First Order Ionosphere Error Mitigation

$$\rho_f^{SV} = r^{SV} + \underbrace{\underbrace{\delta r^{SV}}_{\text{Orbit error}} + \underbrace{T^{SV}}_{\text{Tropo}} + \underbrace{c\left(\delta t_{RX} - \delta t^{SV}\right)}_{\text{Clock error}}}_{\text{Non-dispersive error}} + \underbrace{\underbrace{I_f^{SV}}_{\text{Iono}} + \underbrace{c\left(b_{RX,f} + b_f^{SV}\right)}_{\text{Hardware bias}} + \underbrace{M_f^{SV}}_{\text{Multipath}}}_{\text{Dispersive error}} + \varepsilon_f^{SV}$$

Differencing measurements from two frequencies:

$$\Delta\rho^{SV} = \Delta I^{SV} + c\left(\Delta b_{RX} + \Delta b^{SV}\right) + \Delta\varepsilon$$

Differential Code Biases (DCBs)

Global Ionosphere Map (GIM):

- Network of dual frequency receivers distributed around the globe
- Some receiver DCBs are calibrated
- Antenna installations minimize multipath impact
- Multiple measurement epochs are used to solve for TEC and SV DCBs

NGS TEC map:

- National CORS measurements

A TEC Spatial Gradient-Based Algorithm

$$VTEC_{IPP} = VTEC_0 + \frac{\partial VTEC}{\partial \lambda}\Delta\lambda_{IPP} + \frac{\partial VTEC}{\partial \varphi}\Delta\varphi_{IPP} + O(\Delta\lambda_{IPP}, \Delta\varphi_{IPP})$$

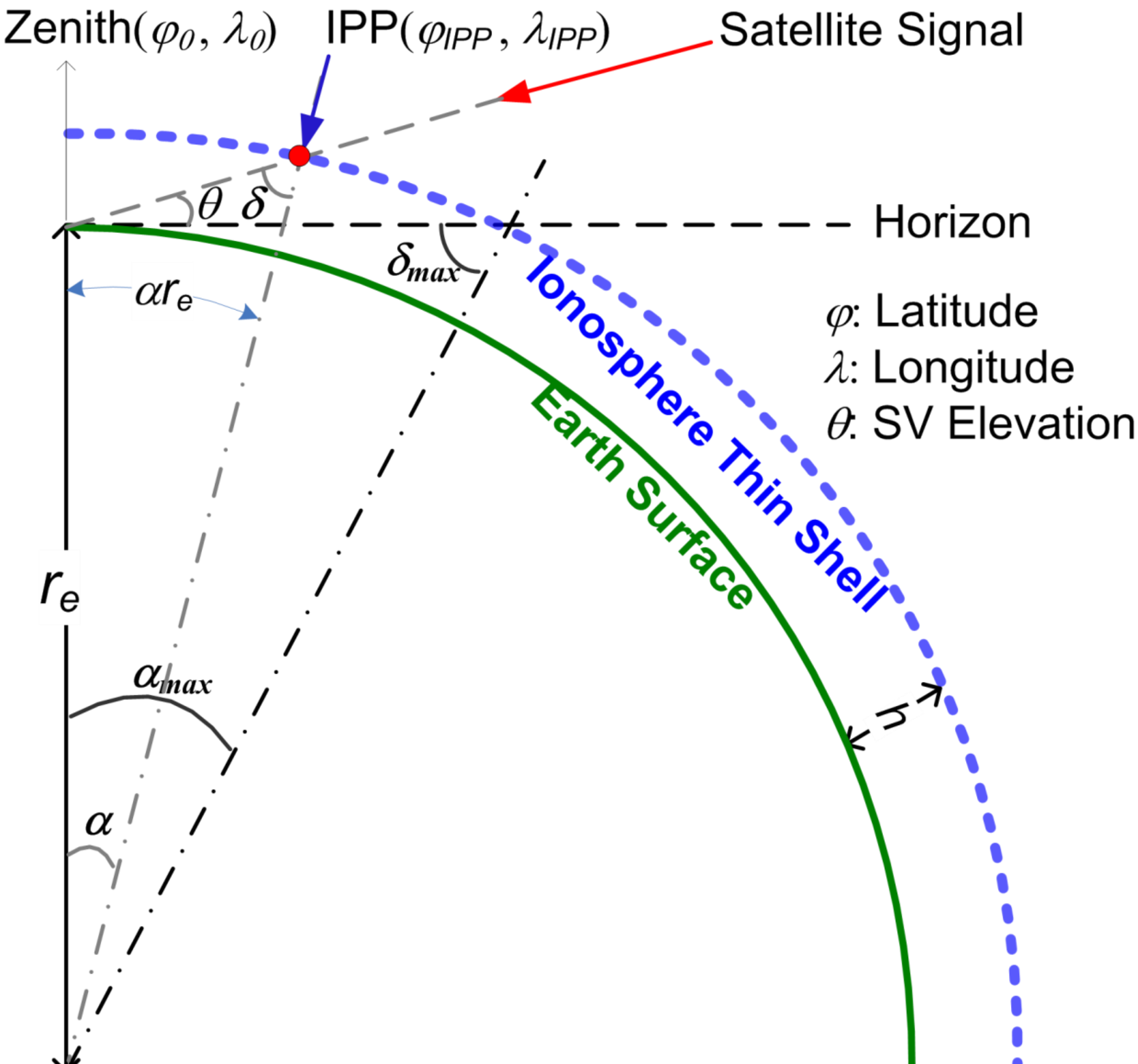

Higher order TEC spatial derivatives

$$\Delta\varphi_{IPP} = \varphi_{IPP} - \varphi_0$$

$$\Delta\lambda_{IPP} = \lambda_{IPP} - \lambda_0$$

$$STEC_{IPP} = VTEC_{IPP} \times MF$$

MF: mapping function

$$I_f^{SV} = 40.3\frac{STEC_{IPP}}{f^2}$$

How Sound Is the TEC Spatial Gradient Assumption?

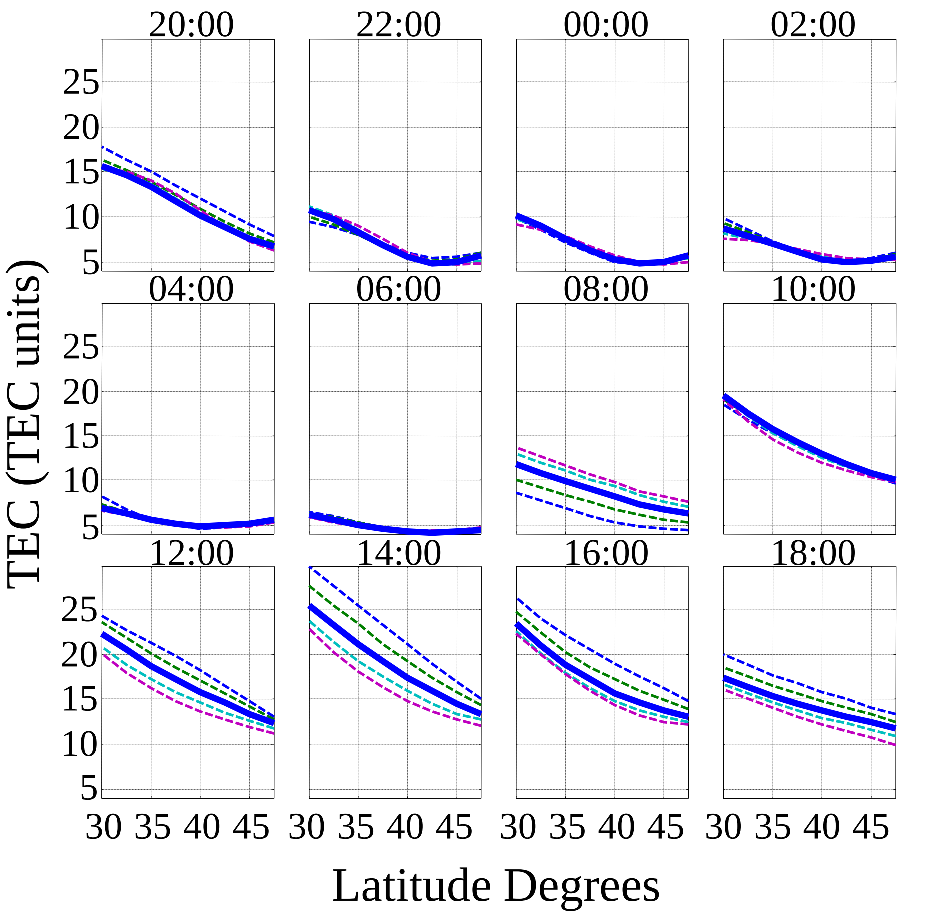

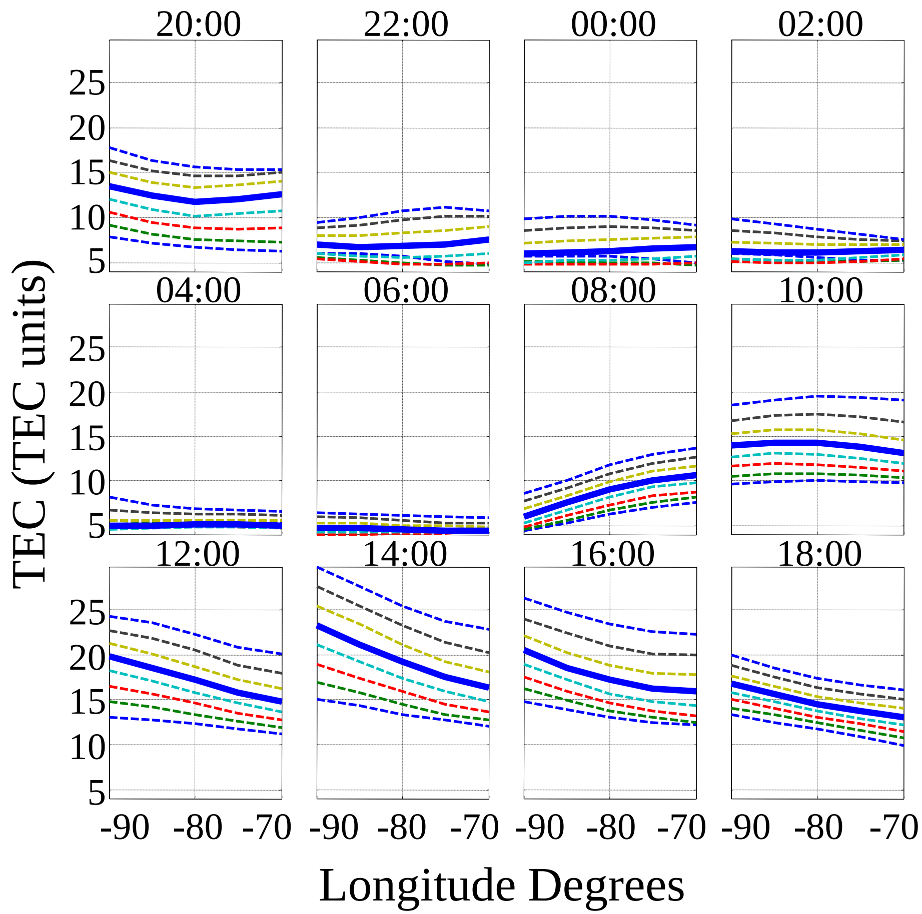

Oxford, OH 3/24/2011

Algorithm Description

$$\Delta\rho^{SV} = \beta \times MF \times \left(VTEC_0 + \frac{\partial VTEC}{\partial \lambda} \Delta\lambda_{IPP}^{SV} + \frac{\partial VTEC}{\partial \varphi} \Delta\varphi_{IPP}^{SV} \right) + c\left(\Delta b_{RX} + \Delta b^{SV}\right)$$

At time epoch k, there are N_k satellites in view → N_k equations, 4+N_k unknowns.

Maximum total number of unknowns from K epochs: 3K+33

Total number of equations: $\sum_{k=1}^{K} N_k$

$$\begin{bmatrix} g_k^{SV(1)} & g_k^{SV(1)}\Delta\lambda_{IPPk}^{SV(1)} & g_k^{SV(1)}\Delta\varphi_{IPPk}^{SV(1)} & 1 & \delta_{1,1} & \cdots & \delta_{1,m} & \cdots & \delta_{1,32} \\ \vdots & \vdots & \vdots & \vdots & \vdots & \vdots & \vdots & \vdots & \vdots \\ g_k^{SV(n)} & g_k^{SV(n)}\Delta\lambda_{IPPk}^{SV(n)} & g_k^{SV(n)}\Delta\varphi_{IPPk}^{SV(n)} & 1 & \delta_{n,1} & \cdots & \delta_{n,m} & \cdots & \delta_{n,32} \\ \vdots & \vdots & \vdots & \vdots & \vdots & \vdots & \vdots & \vdots & \vdots \\ g_k^{SV(N_k)} & g_k^{SV(N_k)}\Delta\lambda_{IPPk}^{SV(N_k)} & g_k^{SV(N_k)}\Delta\varphi_{IPPk}^{SV(N_k)} & 1 & \delta_{N_k,1} & \cdots & \delta_{N_k,m} & \cdots & \delta_{N_k,32} \end{bmatrix} \begin{bmatrix} x_k \\ y_k \\ z_k \\ \Delta b_{RX} \\ \Delta b^{PRN1} \\ \vdots \\ \Delta b^{PRN32} \end{bmatrix} = \frac{1}{c} \begin{bmatrix} \Delta\rho_k^{SV(1)} \\ \vdots \\ \Delta\rho_k^{SV(n)} \\ \vdots \\ \Delta\rho_k^{SV(N_k)} \end{bmatrix}$$

$$\beta = 40.3 \frac{f_{L2}^2 - f_{L1}^2}{f_{L1}^2 f_{L2}^2} \quad g = \frac{\beta}{c} \times MF \quad x = VTEC_0 \quad y = \frac{\partial VTEC}{\partial \lambda} \quad z = \frac{\partial VTEC}{\partial \varphi} \quad \delta_{n,m} = \begin{cases} 1 & \text{if } m = SV_n \\ 0 & \text{otherwise} \end{cases}$$

VTEC Comparison With GIM

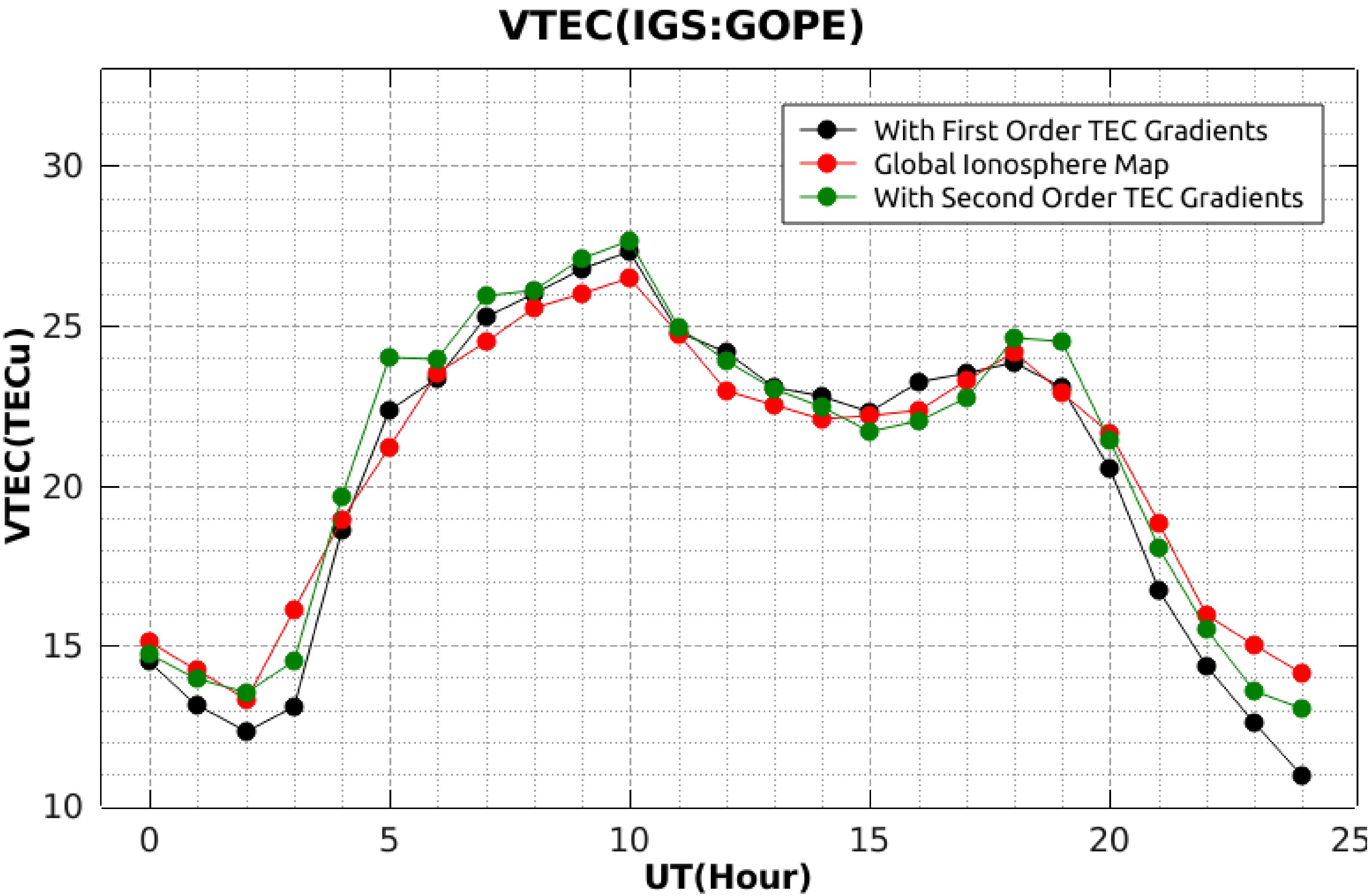

SV and RX DCB Estimation

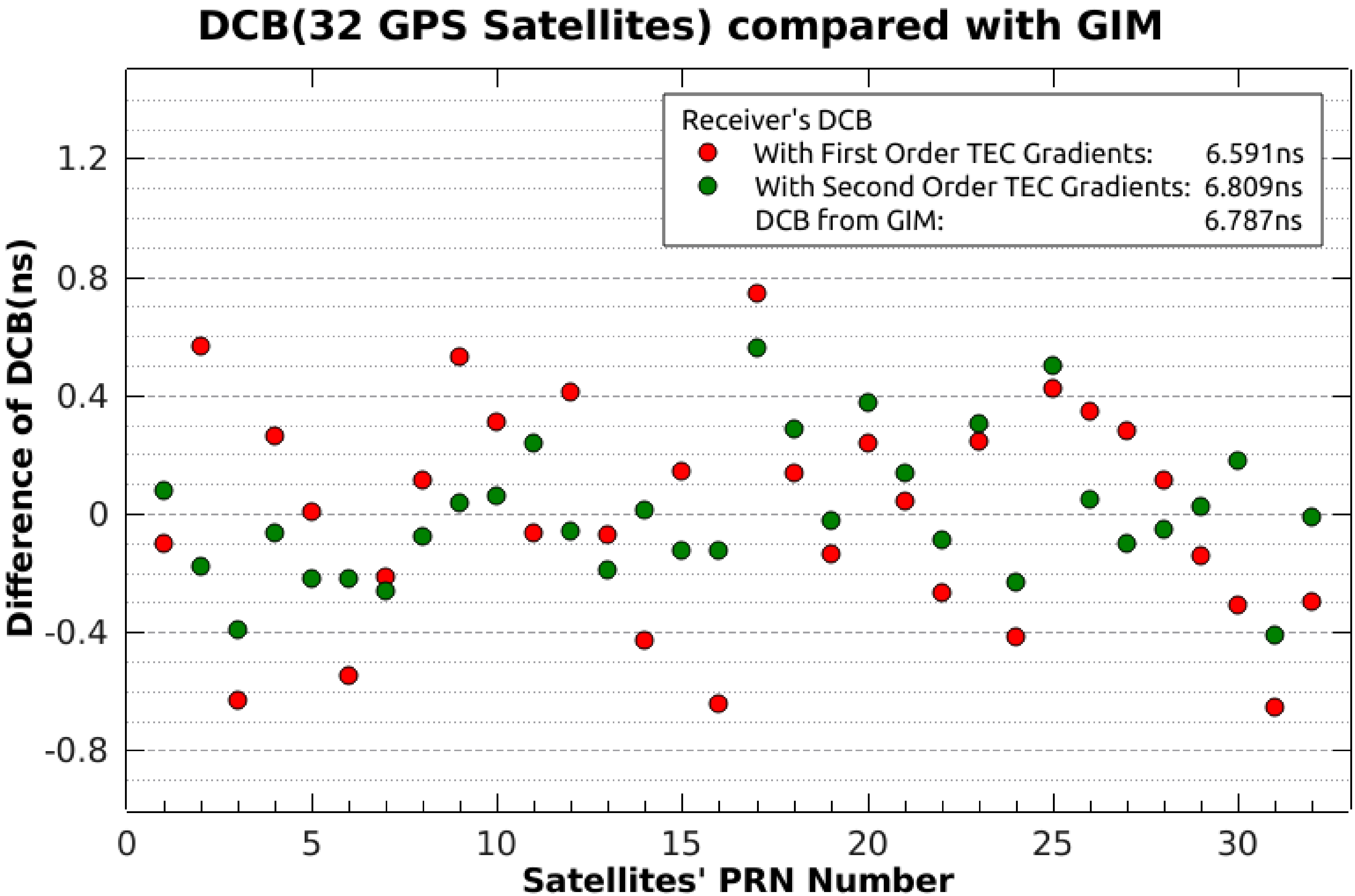

TEC Gradient Solution

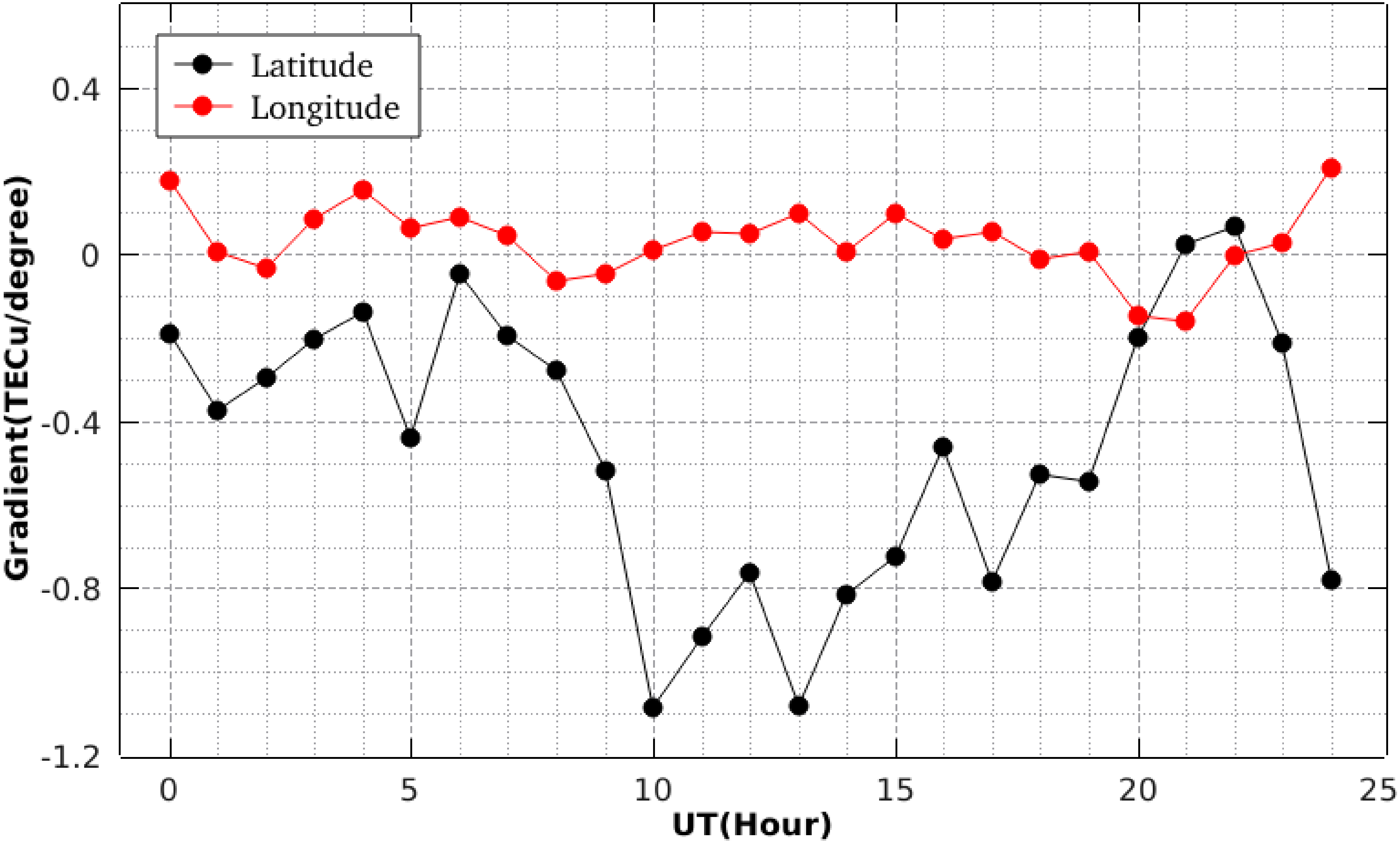

Sparse Network TEC and DCB Estimation

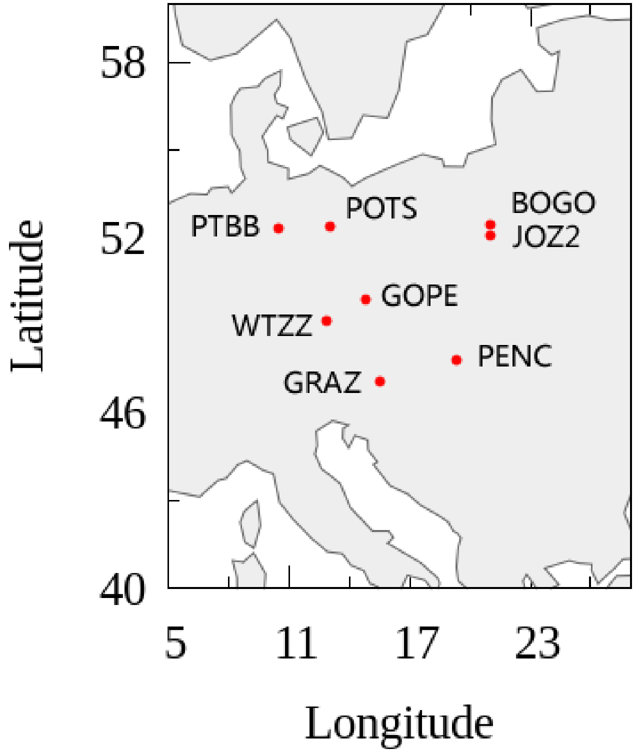

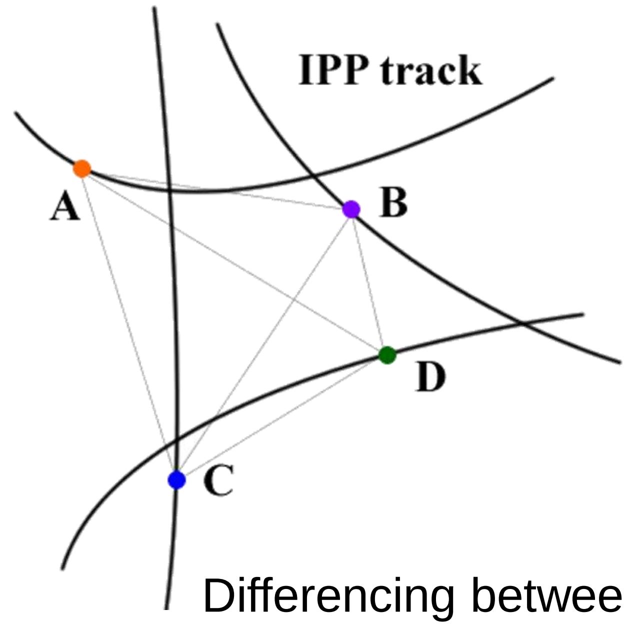

Differencing between IPPs

$$\frac{\Delta\rho_k^{SV(n)}}{c\times g_k^{SV(n)}} = x_k + y_k \Delta\lambda_{IPPk(i)}^{SV(n)} + z_k \Delta\varphi_{IPPk(i)}^{SV(n)} + \frac{\Delta b_{RX(m)} + \Delta b^{SV(n)}}{g_k^{SV(n)}}$$

$n=1,2,\ \ldots,\ N$: SV index for all SVs in view by the network

$m=1,2,\ \ldots,M$: RX index in network

$i=1,2,\ldots,\ I$: IPP index for all RX-SV pairs

Total number of difference equations between 2 IPPs: $I(I-1)/2$

TEC Spatial Gradients From A Sparse Network

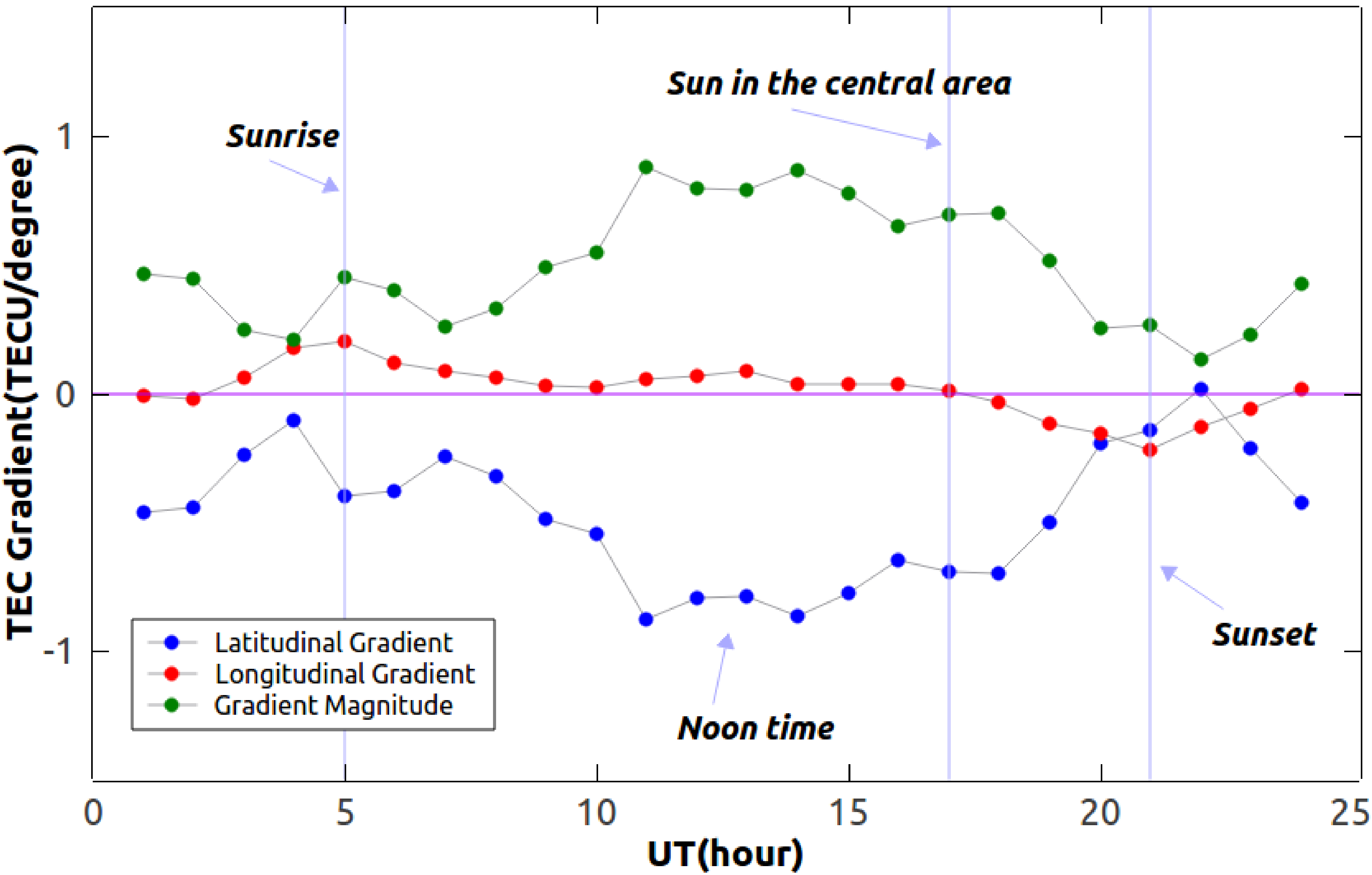

On-Going Efforts in First Order Error Estimation

1. **Use of multi-constellation GNSS measurements**
2. **Joint GNSS receiver and incoherent scatter radar experiments**
3. **Performance evaluations at diverse geographical locations**
4. **Introduce IPP height as a new variable**
5. **Introduce vertical Ne profile dependency**
6. **Introduce RX DCB as a time-varying quantity**
7. **Impact on PPP performance evaluation**

Higher Order Ionosphere Error

Rough Estimation of Iono Error

TEC: 60 units (1 unit=10^{16} el/m^2)

$$q = 40.3TEC$$

1st order: $\boxed{\dfrac{q}{f^2} = 10m}$

B_0: ~ 30000nT TEC:60units

$$s = 7527c\int N_e B_0 \cos\theta_B dl \le 7527cB_0\int N_e dl = 7527cB_0 TEC$$

2nd order: $\boxed{\dfrac{s}{f^3} \approx 1cm}$

B_0: ~ 30000nT TEC:60units Uniform Ne in ΔL: 100km

$$r_1 = 2437\int N_e^2 dl \approx 2437 N_e^2 \Delta L \approx 2437\frac{TEC^2}{\Delta L}$$

3rd order: $\boxed{\dfrac{r_1}{f^4} \approx 1mm}$ + $\boxed{\dfrac{r_2}{f^4} \approx 0.01mm}$

$$r_2 = 4738\times10^{22}\int N_e B_0^2\left(2+\cos^2\theta_B\right)dl \le 10^{26} B_0^2 TEC$$

How To Accurately Estimate Higher Order Error?

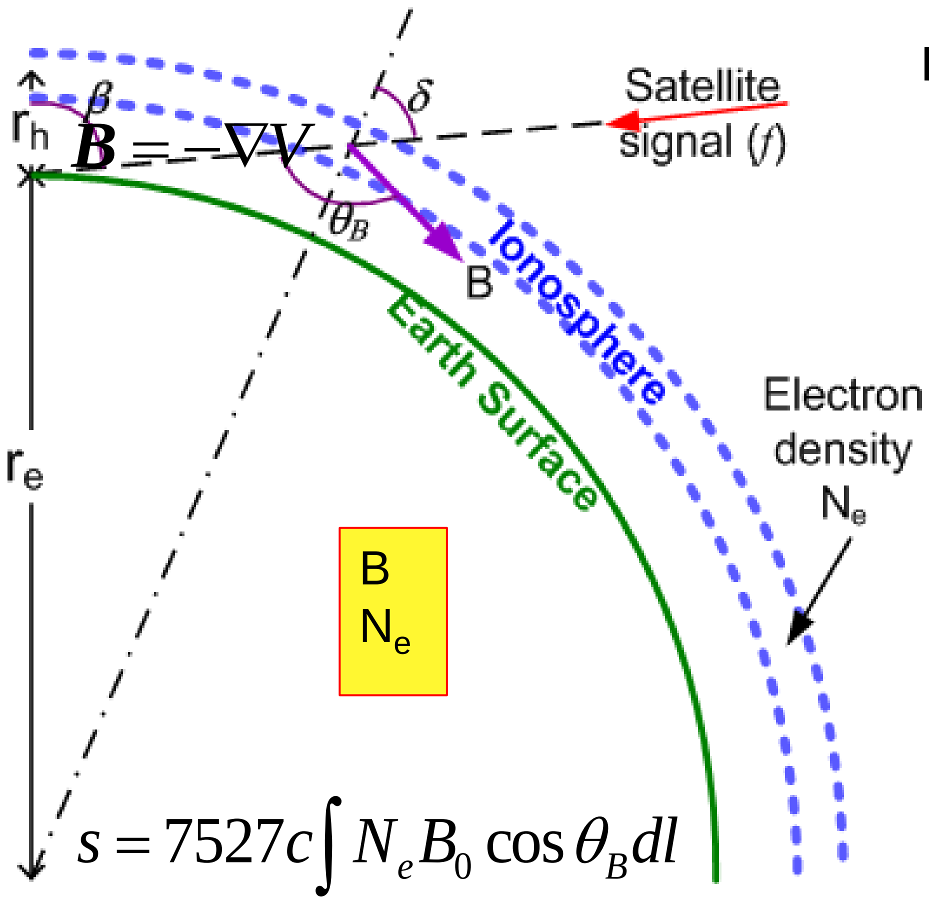

B field:

International Geomagnetic Reference Field (IGRF) model, 11th Generation

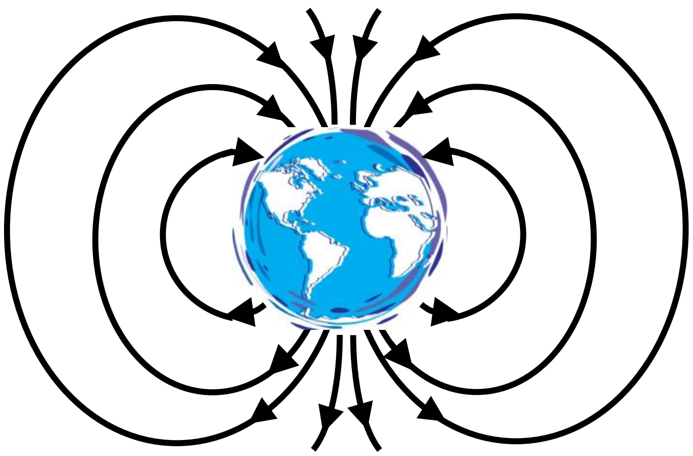

Question:

How good is the model in ionosphere?

IGRF Model Validation

Low Earth Orbit Satellite-Based Magnetometers (100 - 1000 km)
Over 600 GB satellite measurements analyzed

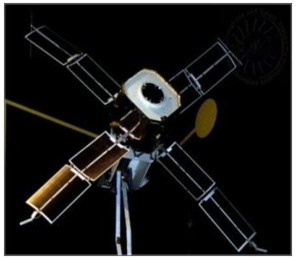

MAGSAT (NASA)
300-600 km altitude
November 2, 1979 – May 6, 1980.

Ørsted (Danish Meteorological Institute)
630 – 860 km altitude
March 1999 – Present

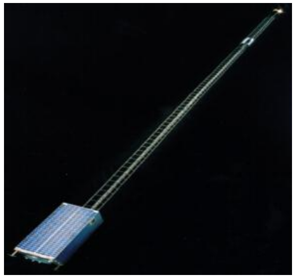

SAC-C (Argentine Commission on Space Activities)
702 km altitude
January 23, 2001 – December 4, 2004

CHAMP (Germany)
350-450 km altitude
May 15, 2001 – Present

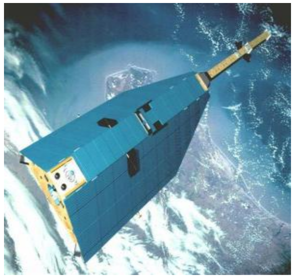

DEMETER (France)
660 – 715 km altitude
August 11, 2004 - Present

11th Generation IGRF Validation Results

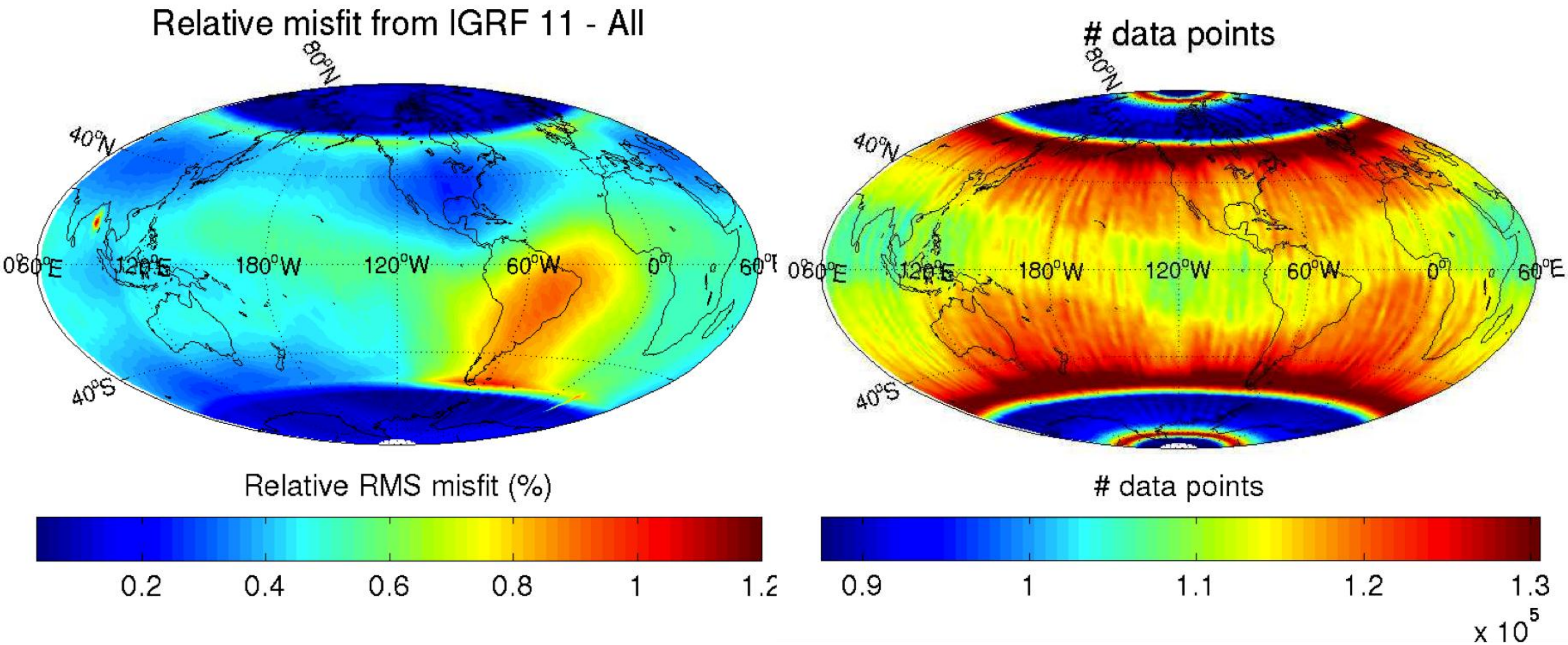

Ne Profiles

Arecibo 1.5MW VHF/UHF Incoherent Scatter Radar
Ne profiling up to 2200km

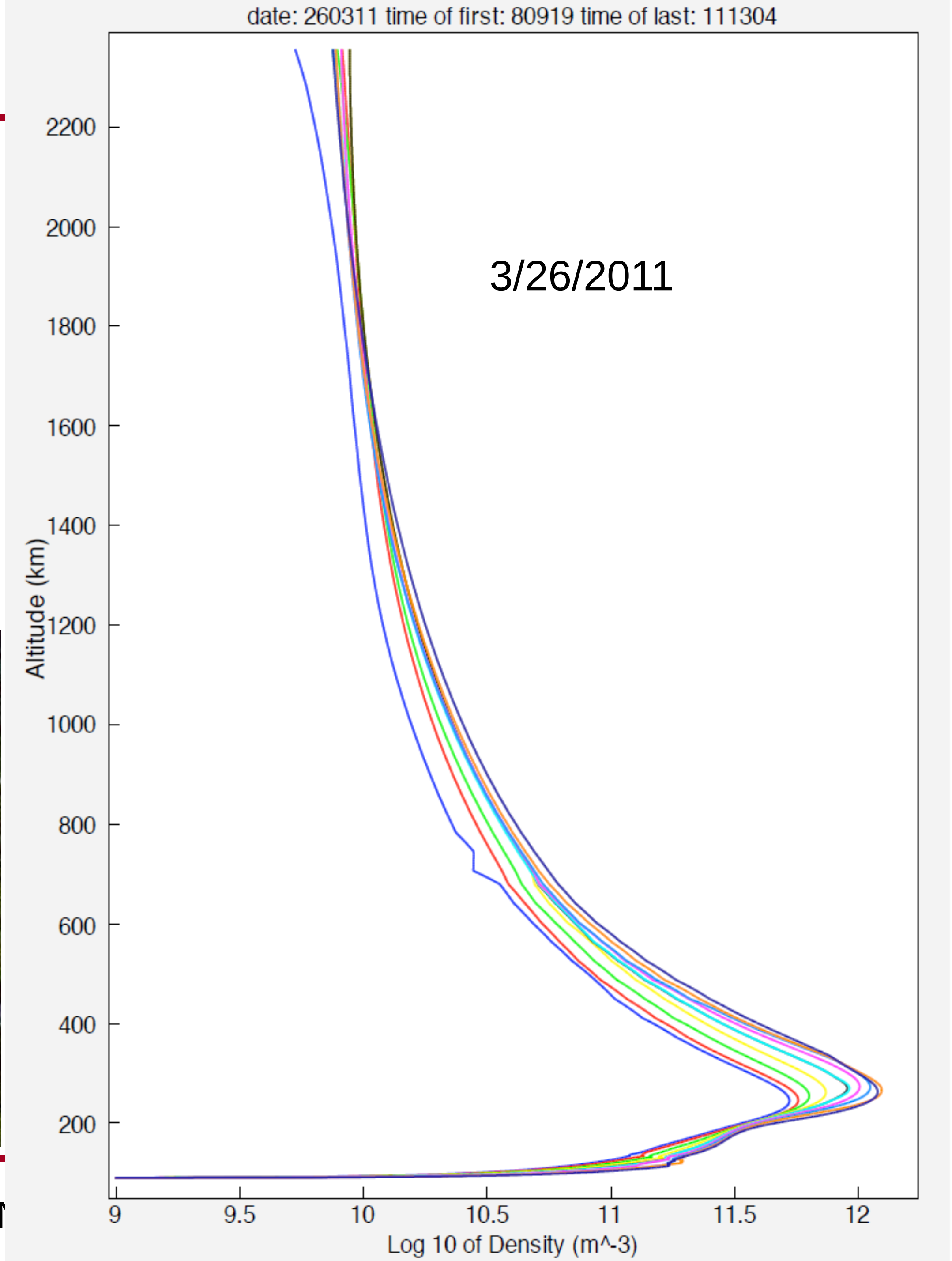

Multiple ISR Measurements

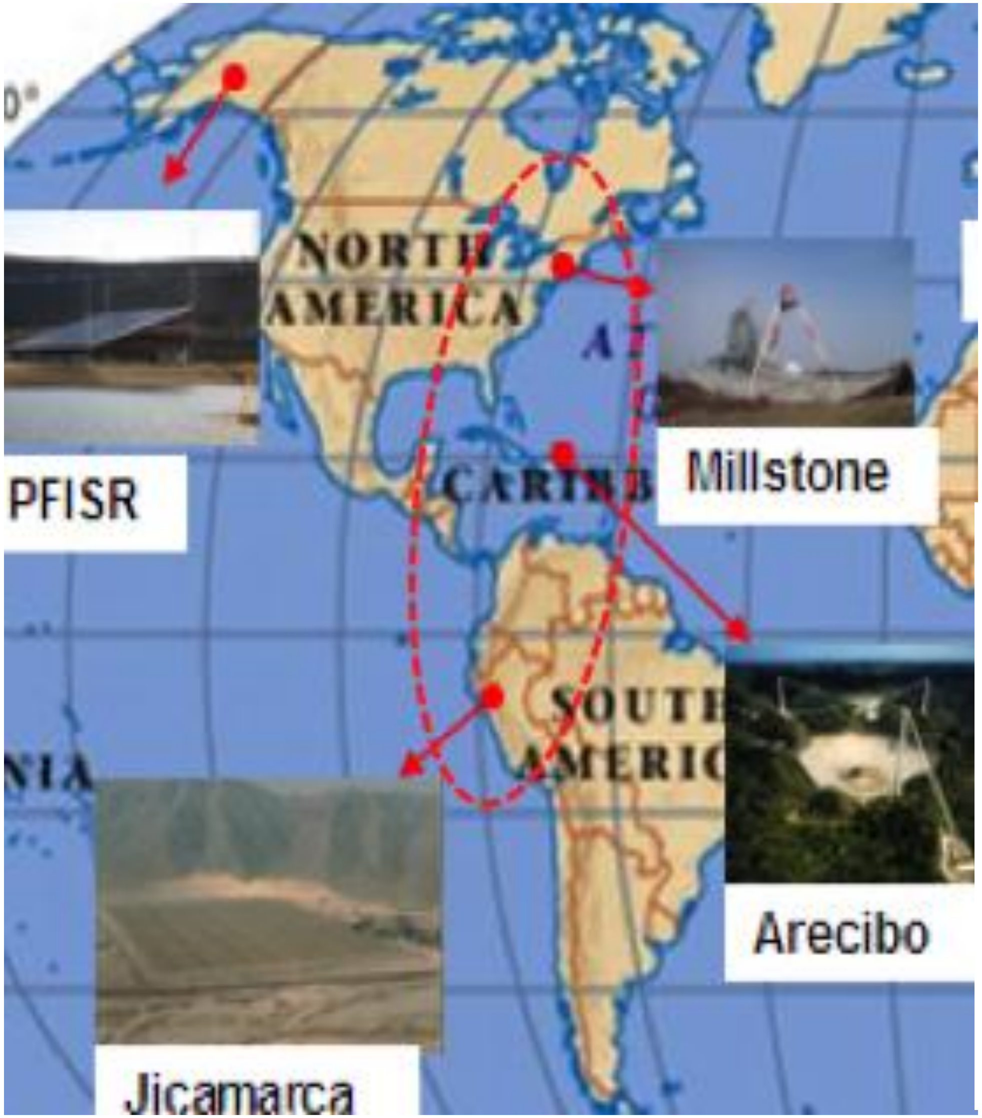

Over 1 decade of data
Daily
Seasonal
Solar activities
Geographical

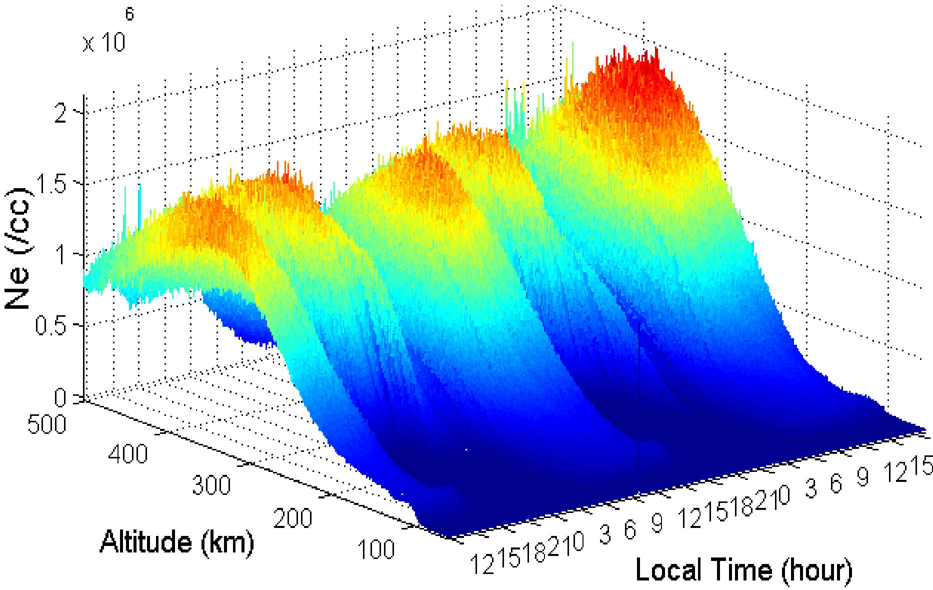

Ionosphere Radio Occultation

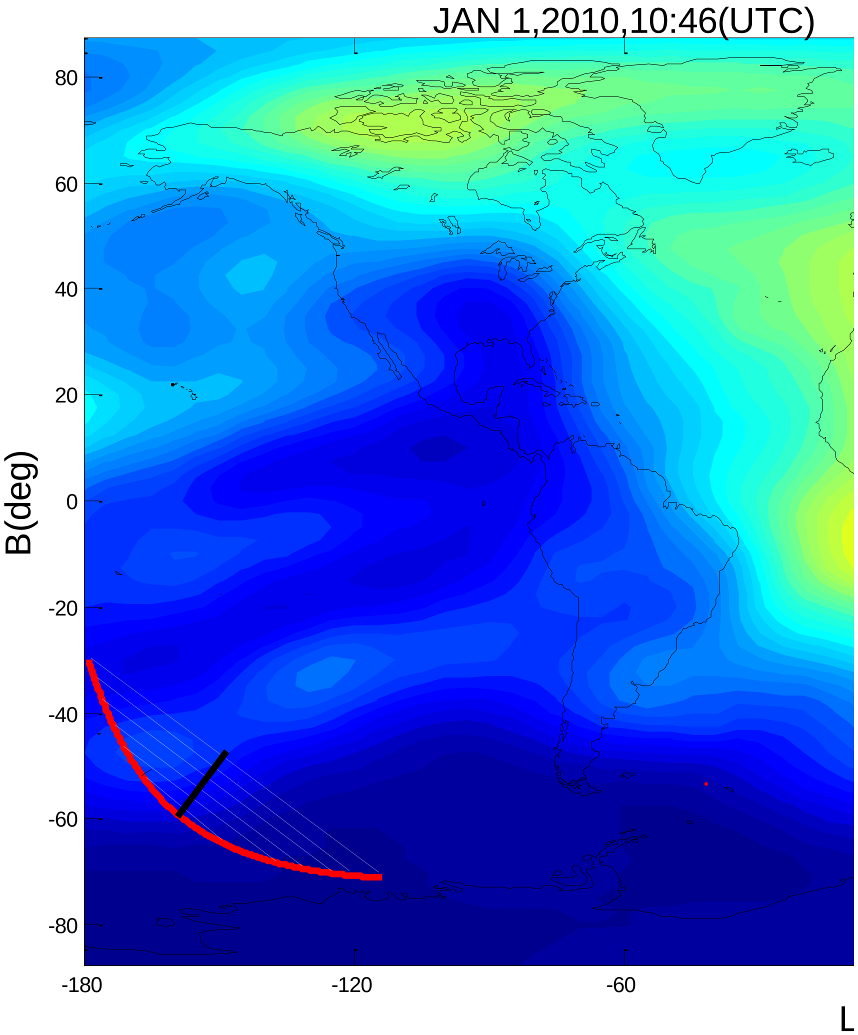

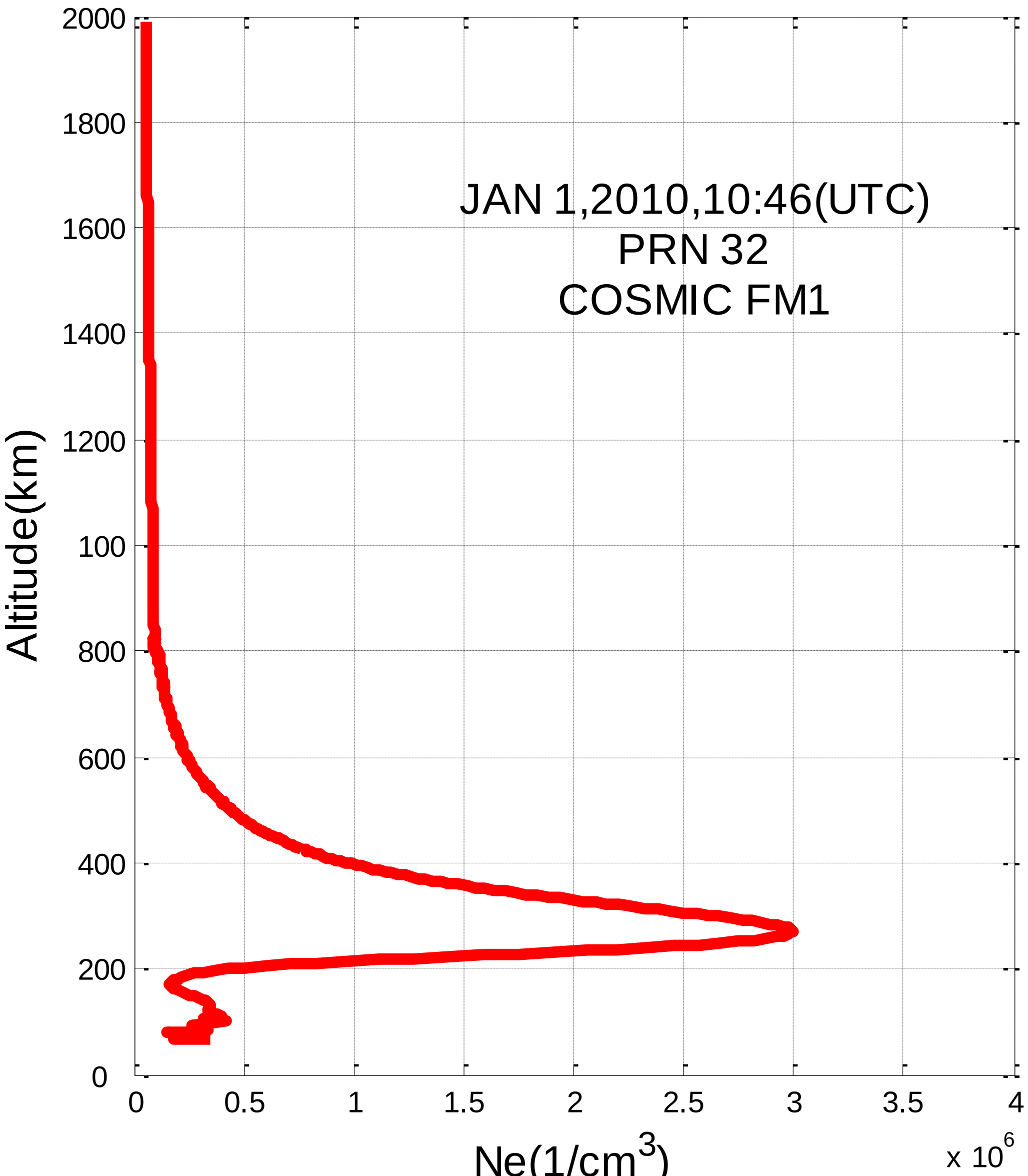

Higher Order Error Spatial Behavior

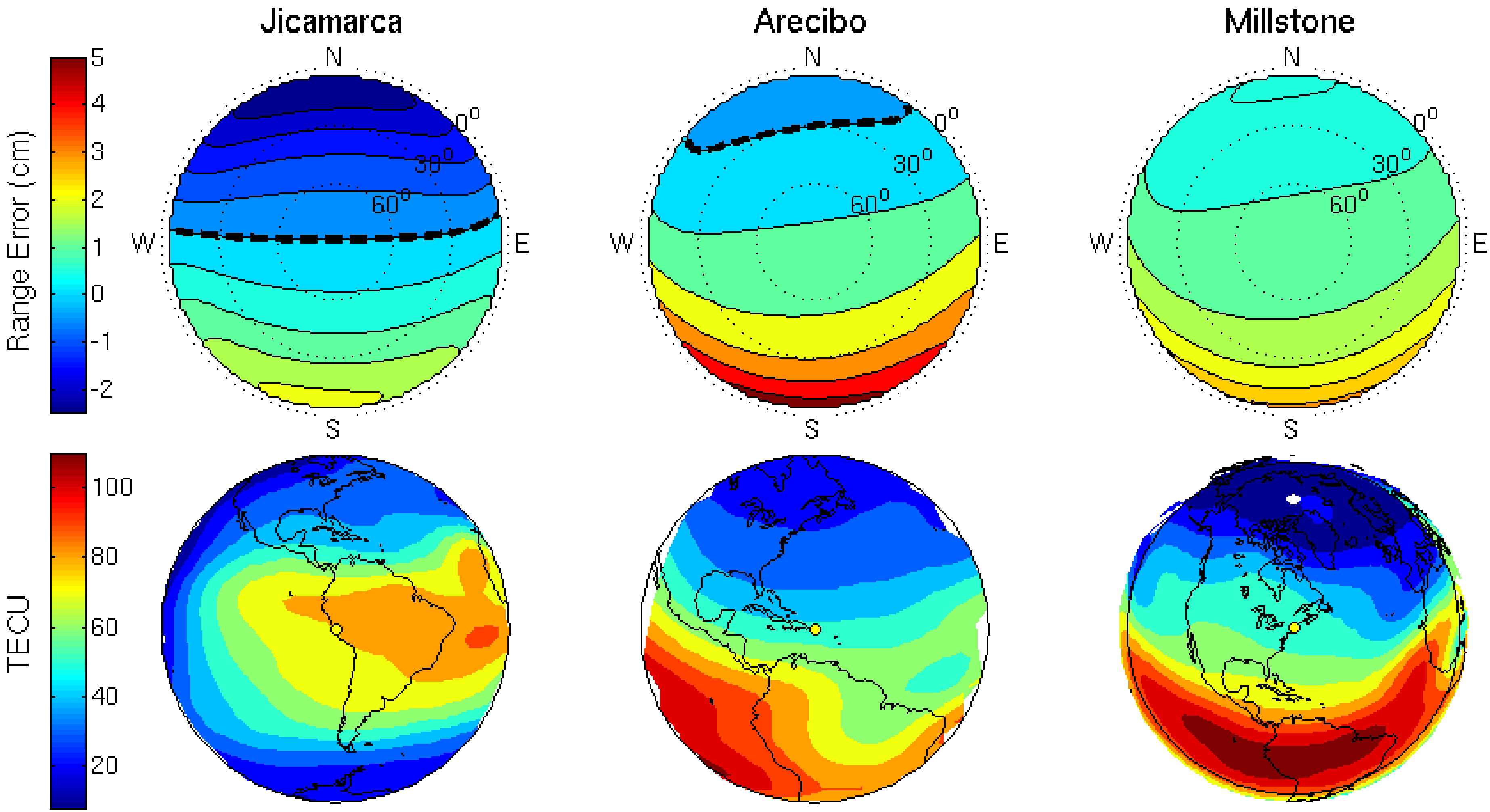

3 December 2002
10:11 AM (local), Kp 2

11 April 1989
5:04 PM (local), Kp 2

17 October 2002
12:30 PM (local), Kp 2

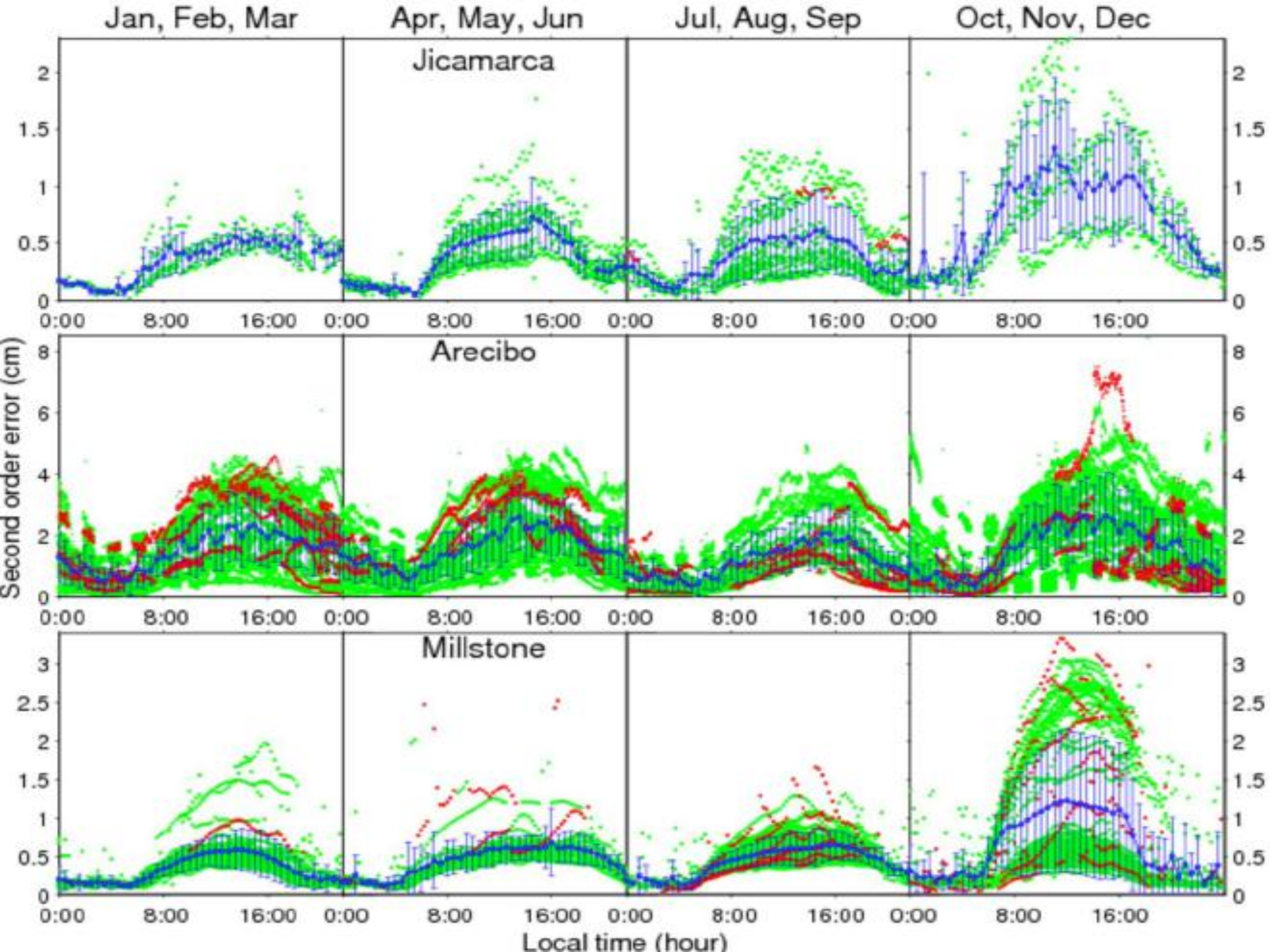

Jan, Feb, Mar
Apr, May, Jun
Jul, Aug, Sep
Oct, Nov, Dec
Jicamarca
Arecibo
Millstone
Second order error (cm)
Local time (hour)
0:00
8:00
16:00

Geomagnetic Activity Impact

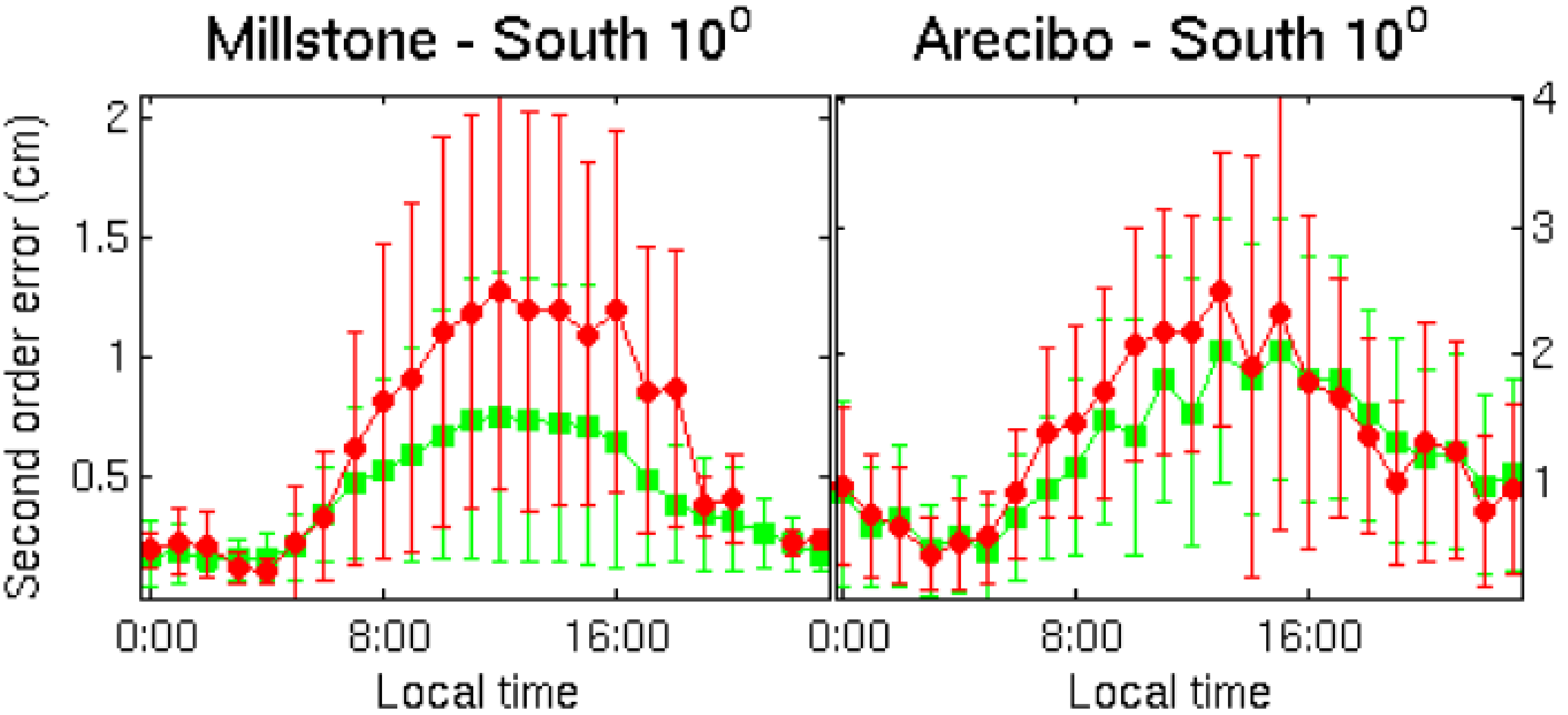

Ionospheric Scintillation

Iono. Scintillation Conceptual Description

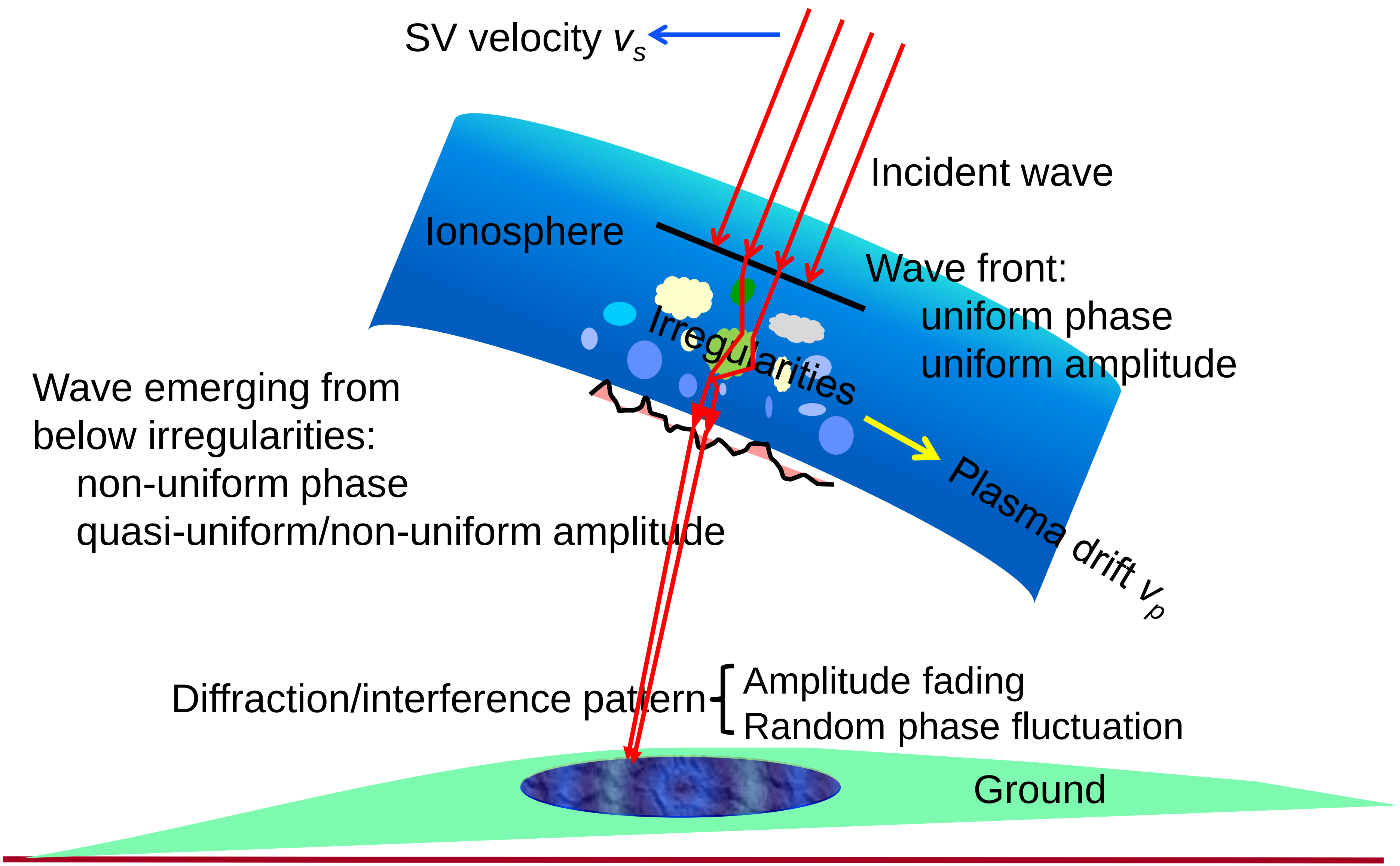

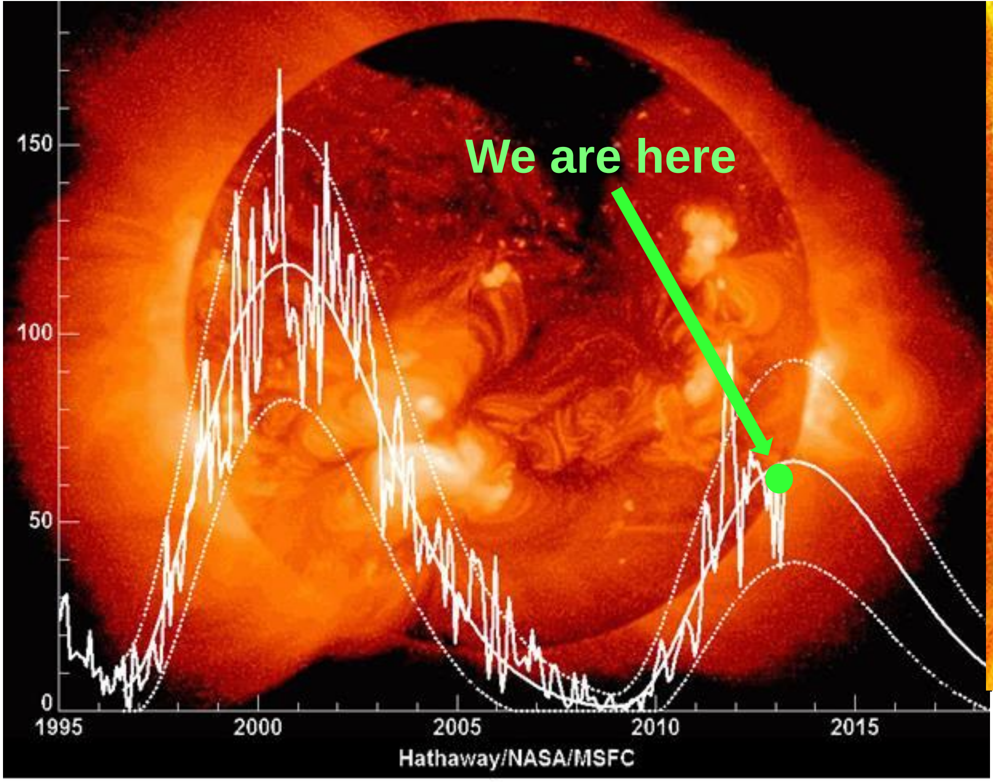

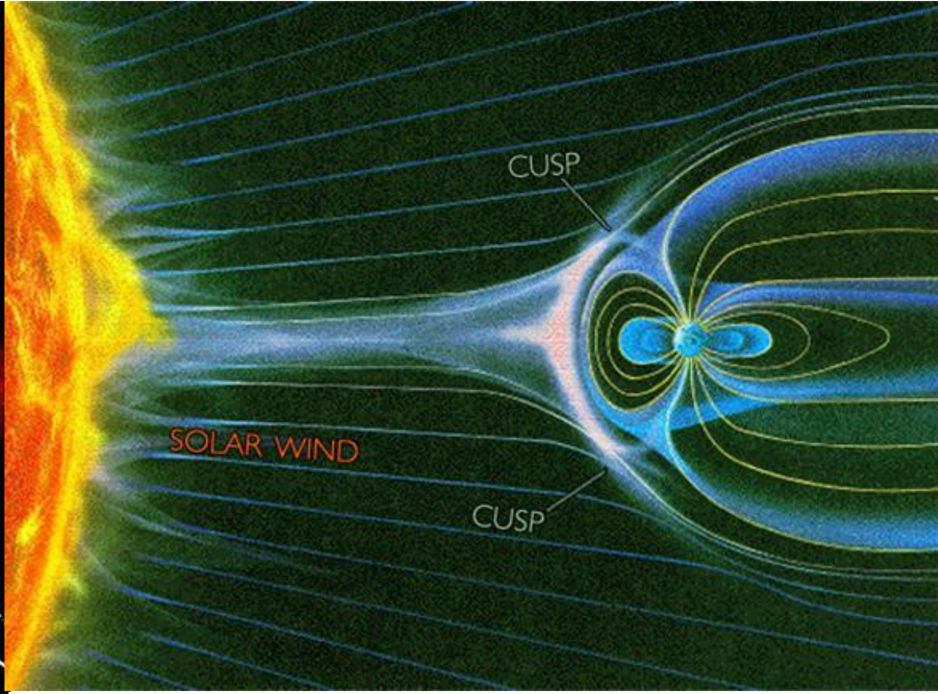

High latitude:
Mainly driven by **solar and magnetosphere** activities

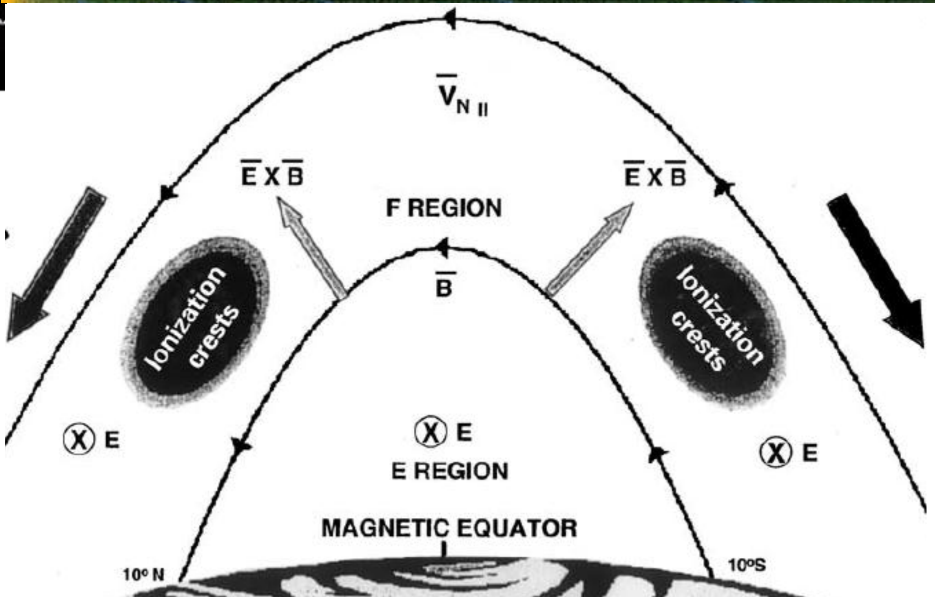

Low latitude:
Ionosphere internal mechanisms
+ modulation by solar activities

Basu, S. et al, "Specification and forecasting of scintillations in communication & navigation links: current status and future plans," J. Atmos. Solar-Terr. Phy., 2002.

Strong Equatorial Scintillation: Simultaneous Deep Fading and Large Phase Fluctuation

03/18/2001 8:45-9:30PM

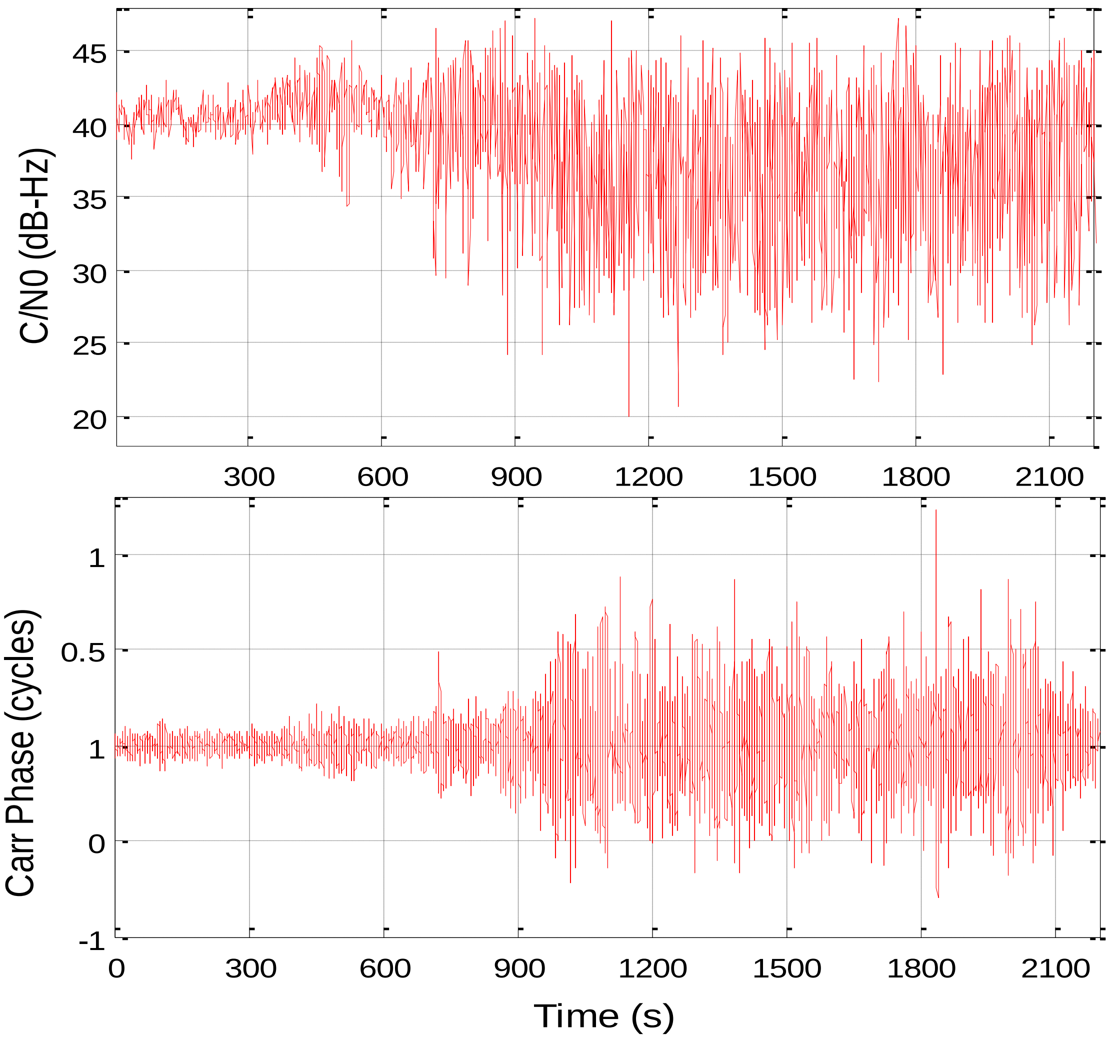

Ascension Island

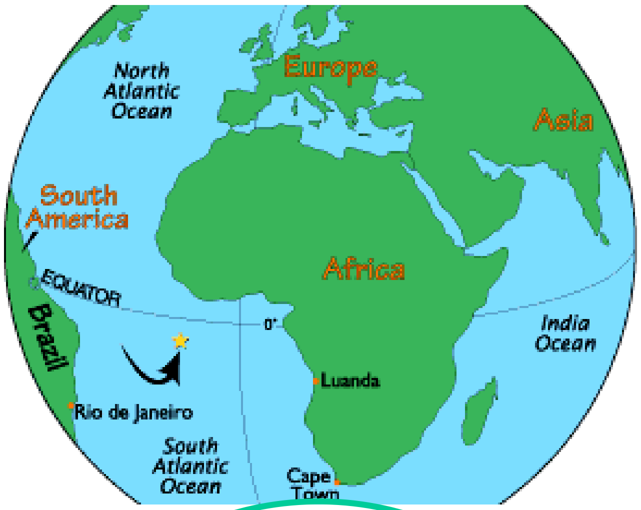

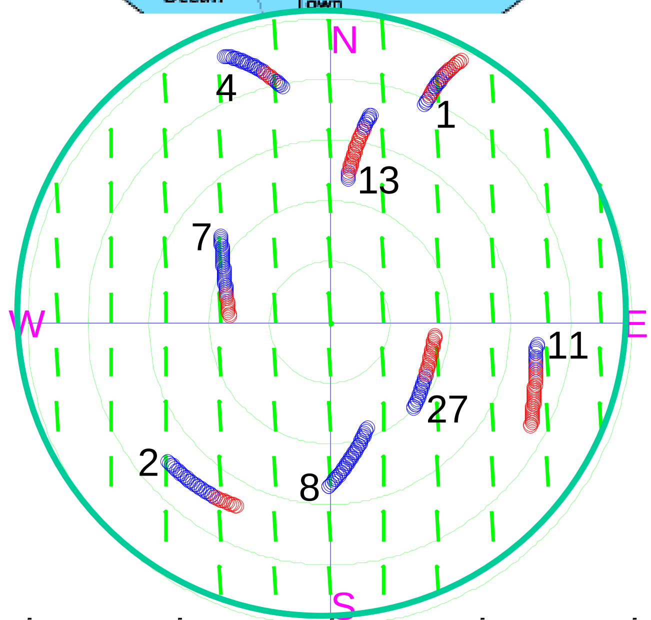

Conflicting Demands on Scintillating GNSS Signal Tracking

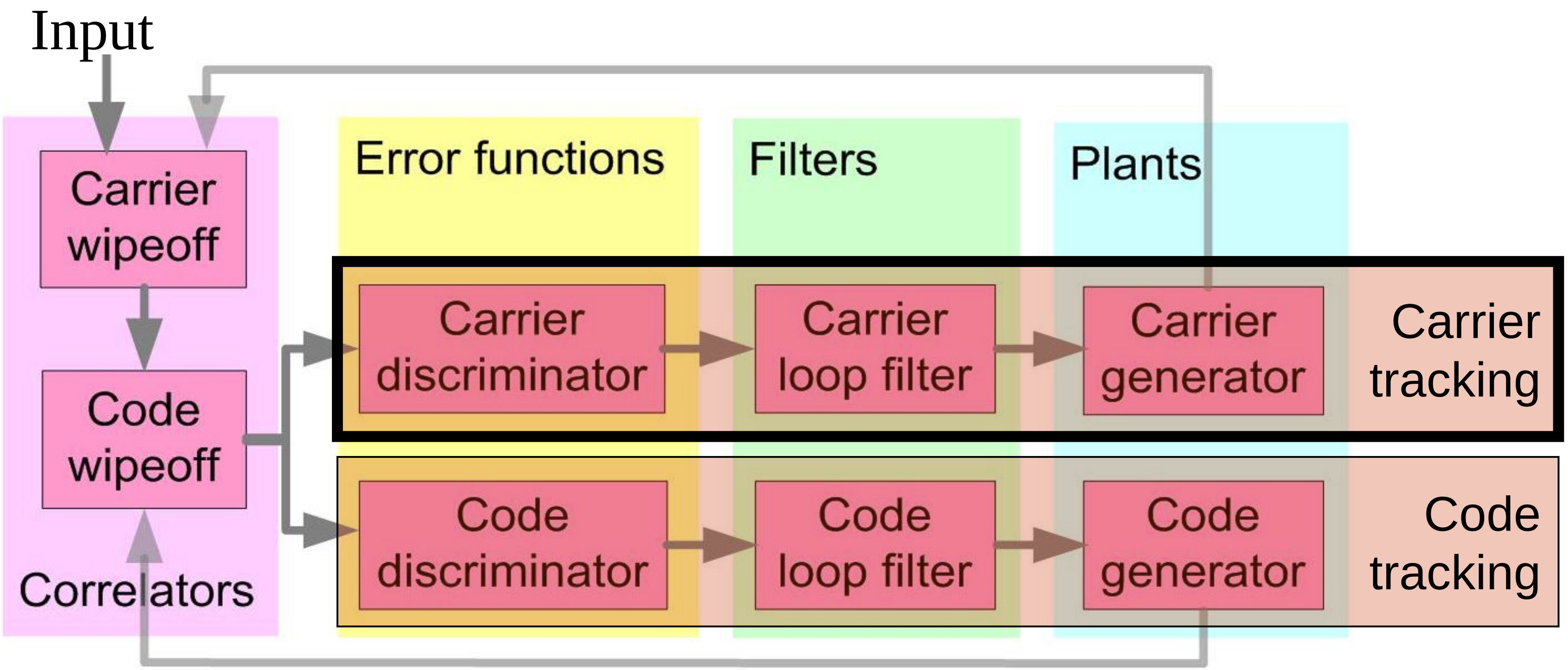

Integration time T_I	Discriminator type $\Delta(\theta)$	Filter BW B	⇐ Tracking parameters
Short	High dynamics	Wide	⇐ High carrier dynamics
Long	High sensitivity	Narrow	⇐ Deep signal fading

Research Objectives

- **Data Collection:** Establish high quality scintillation event monitoring and data collection stations at both high and low latitude scintillation zone.
- **Ionosphere Characterization:** Develop accurate signal parameter estimation techniques to characterize scintillation behavior for ionosphere research and GNSS receiver development.
- **Receiver Algorithms:** Develop robust GNSS tracking algorithms to ensure continuity and accuracy of navigation solutions during space weather events.

Existing GNSS Space Weather Monitoring Systems Issues

1. Commercial GNSS receivers are designed for **PNT** solutions. They are not optimized for **remote sensing** applications.

2. Space weather events are **Nuisances** for PNT. Receiver signal processing will **hide** them → Measurements are **not true** representation of physical processes in space.

3. Receiver design and signal processing are **proprietary**. Users have **no knowledge** of specific processing used.

4. Receivers **break down** during strong space weather events. Critical data cannot be collected when needed most.

High quality, raw GNSS RF data are needed for Ionosphere studies and robust GNSS receiver development

Event Driven Wideband IF Data Collection System

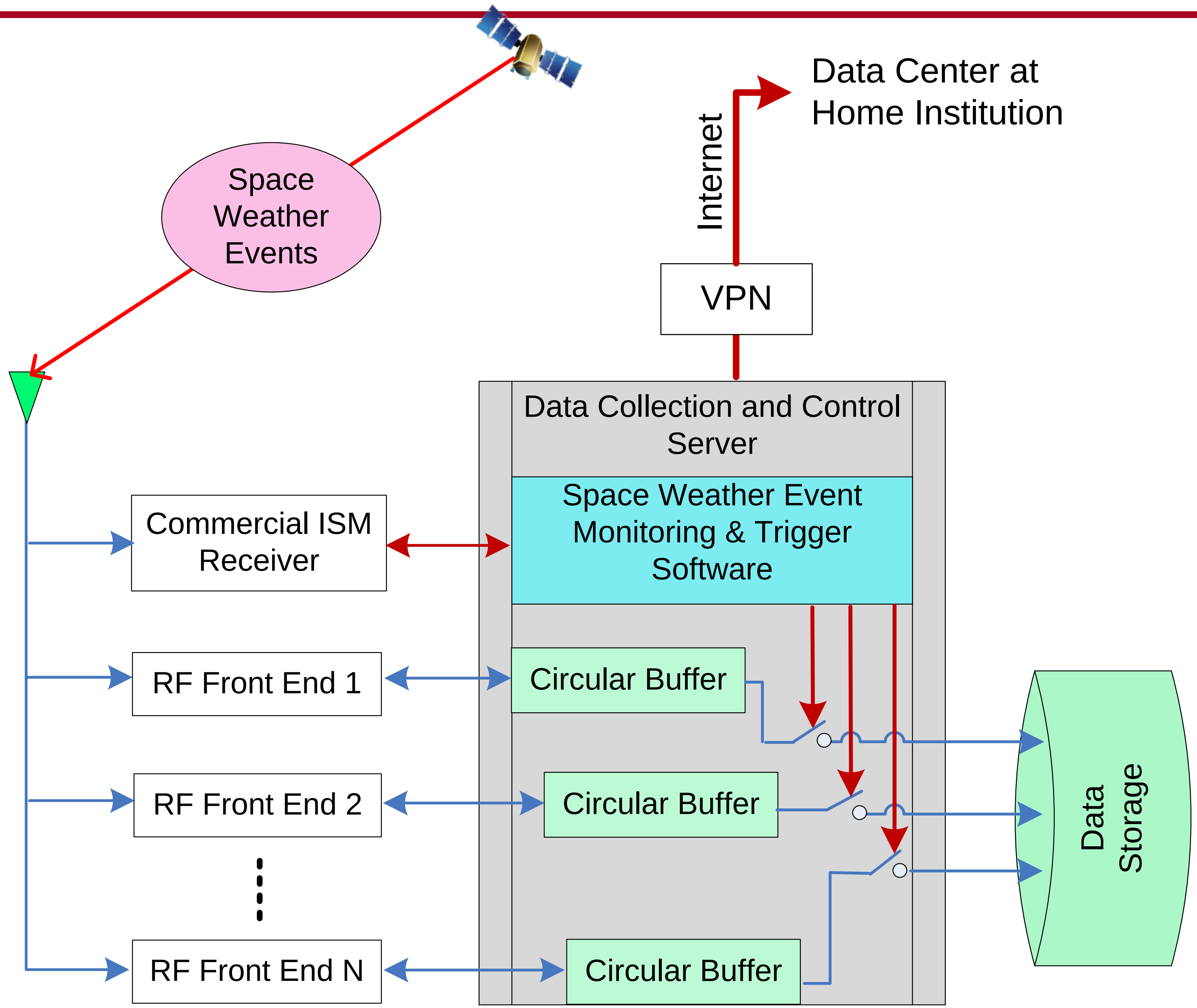

HAARP (Gakona, Alaska)

Lat: 62.39°, Lon: 145.15°W

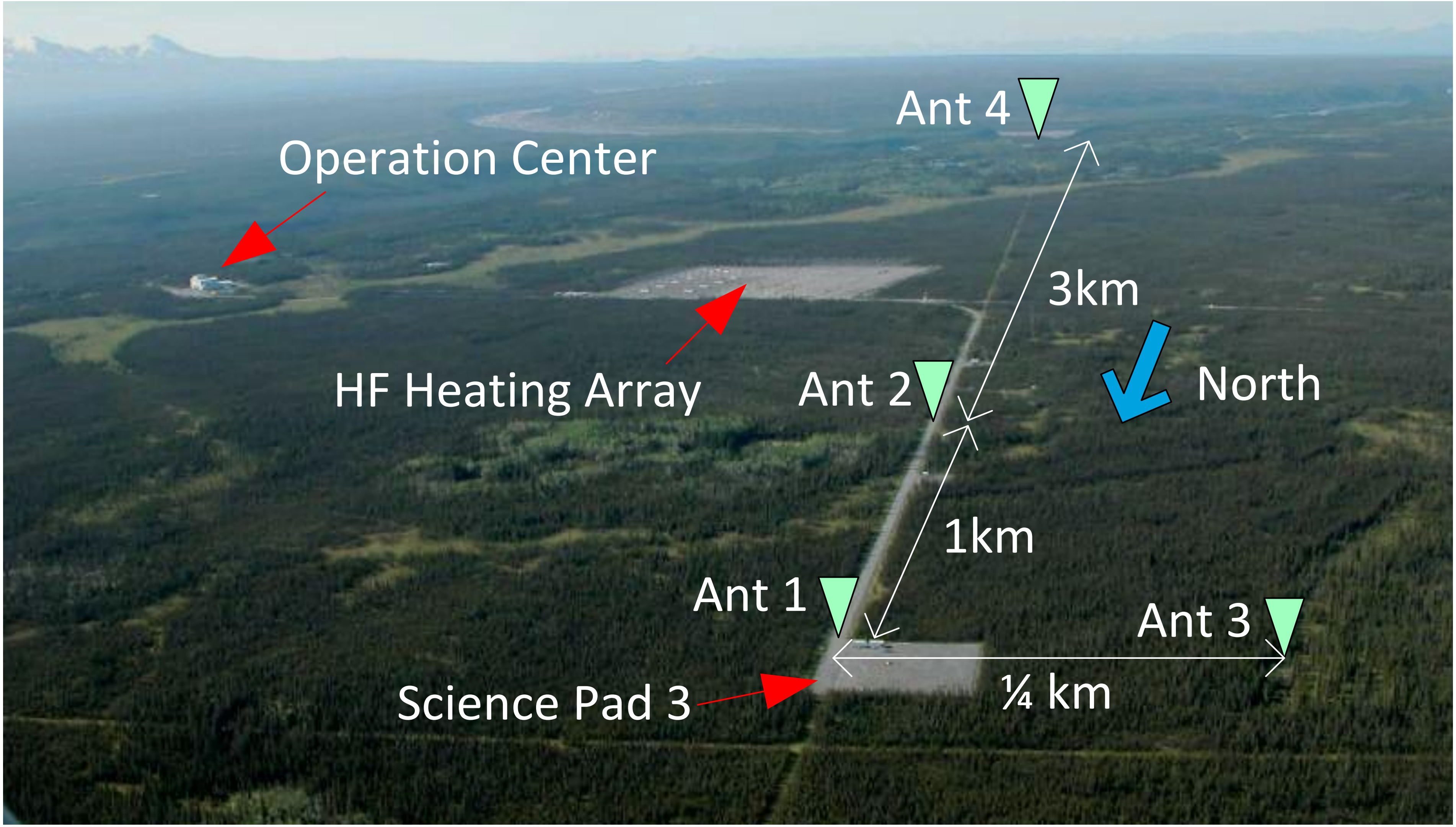

HAARP GNSS Receiver Array

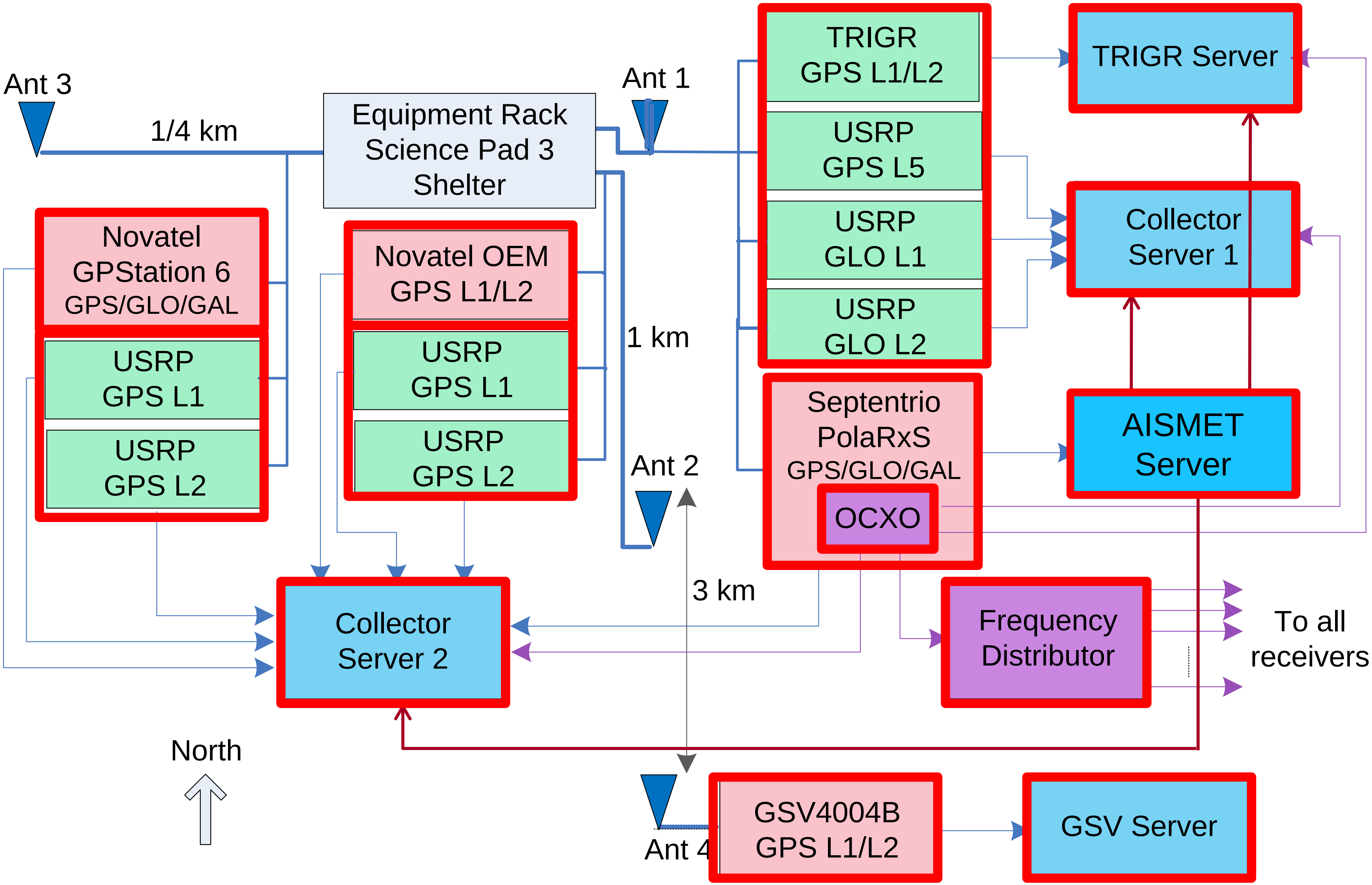

Scintillation Event Trigger Example

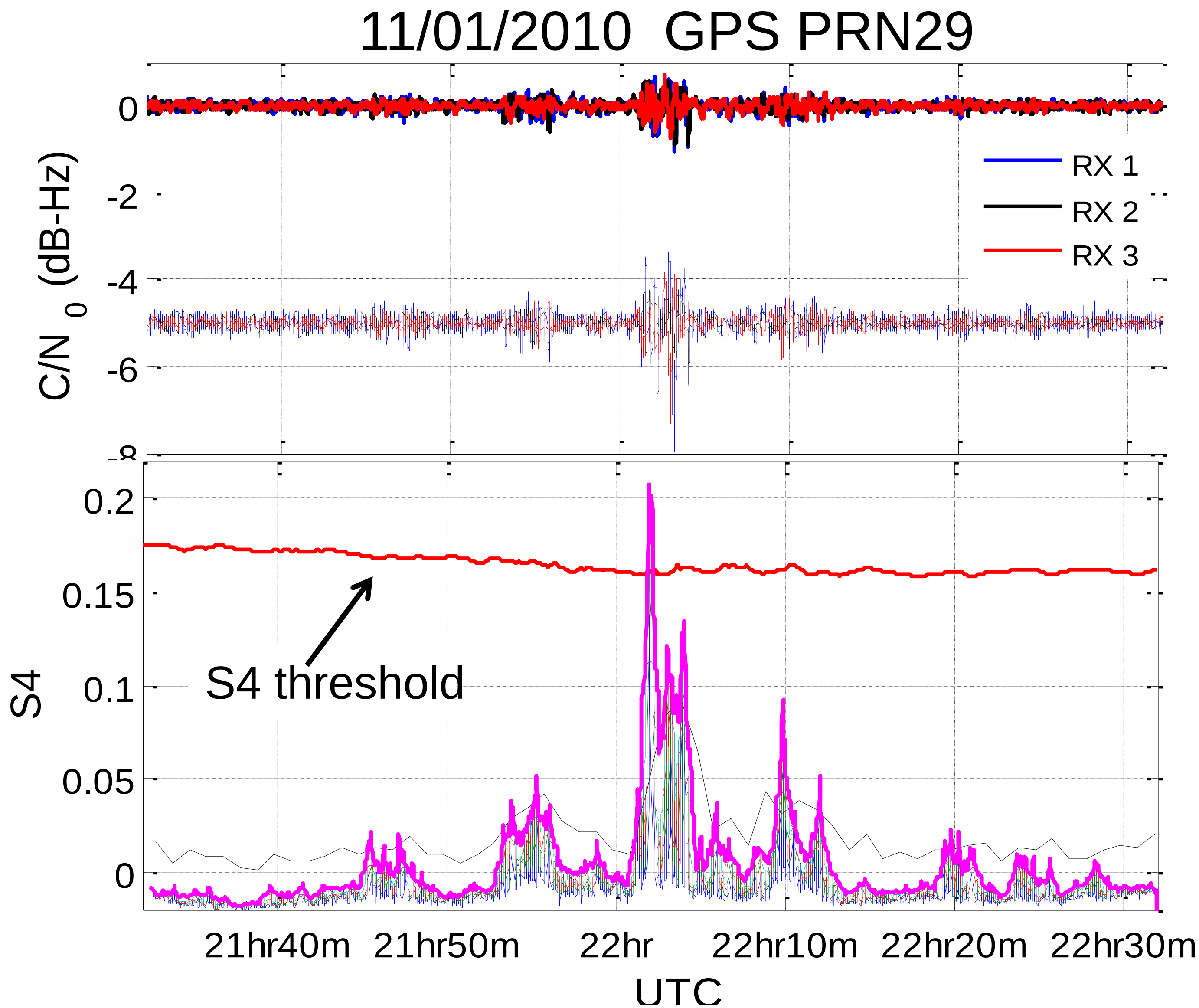

Multi-Constellation GNSS → Spatial Observability

GPS (with L2C)
GLONASS
Galileo
Beidou

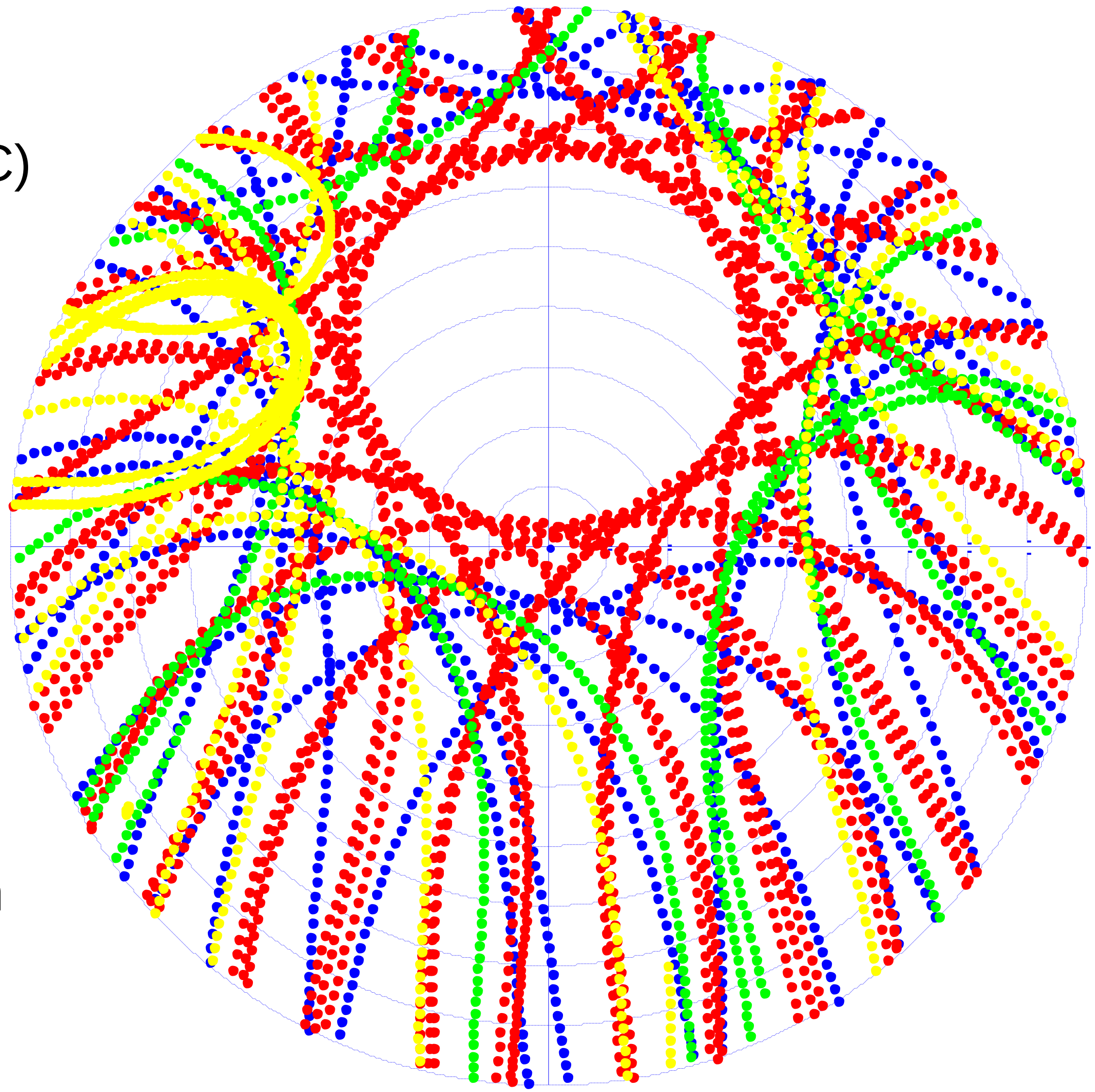

05/19/2013
HAARP, Alaska
(62.39°N,145.15°W)
24-hour satellite path

A New Global GNSS Space Weather Data Collection Network

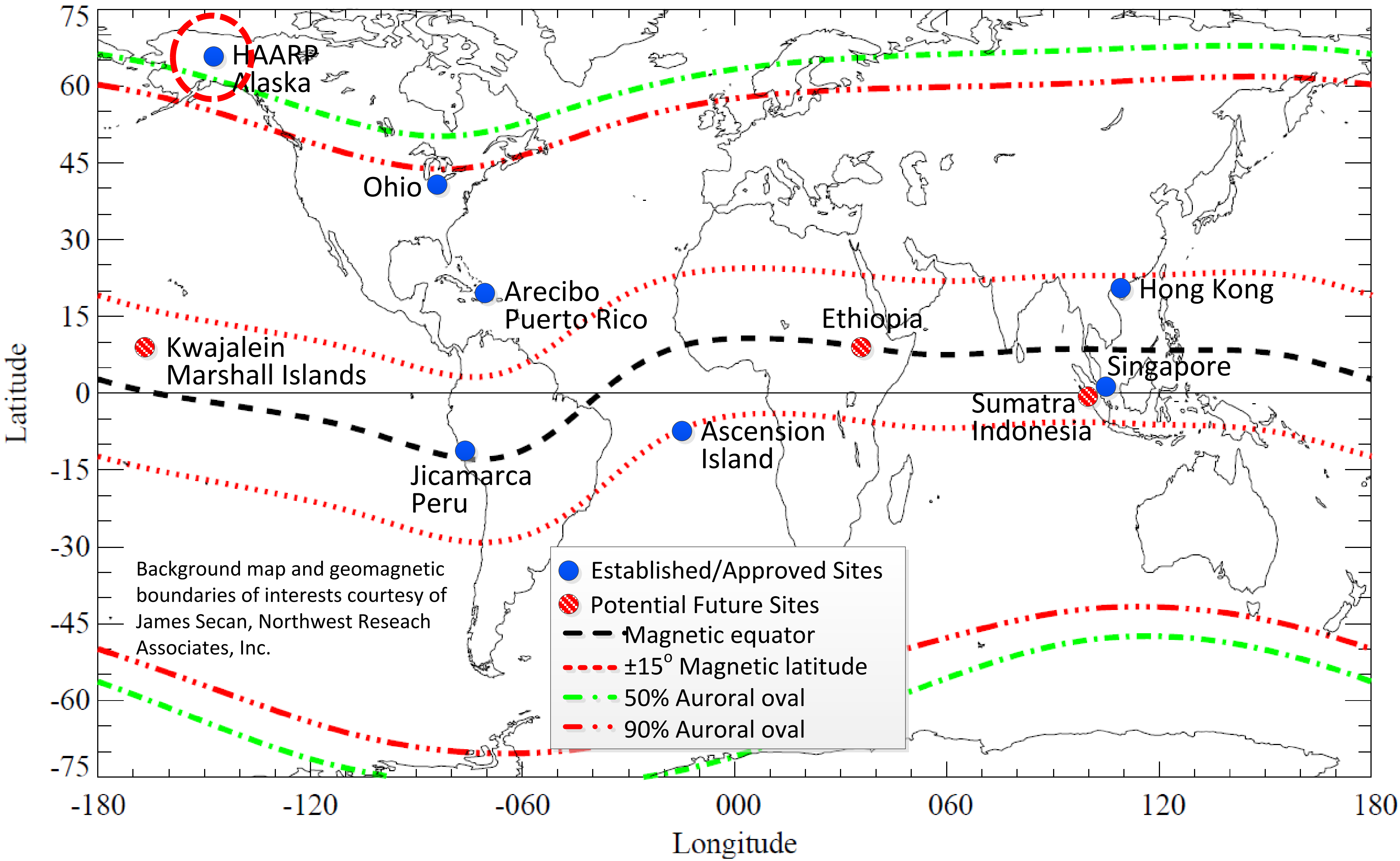

Strategic Site Selection for Collaborative Research

High Latitude Scintillation Spatial Distribution

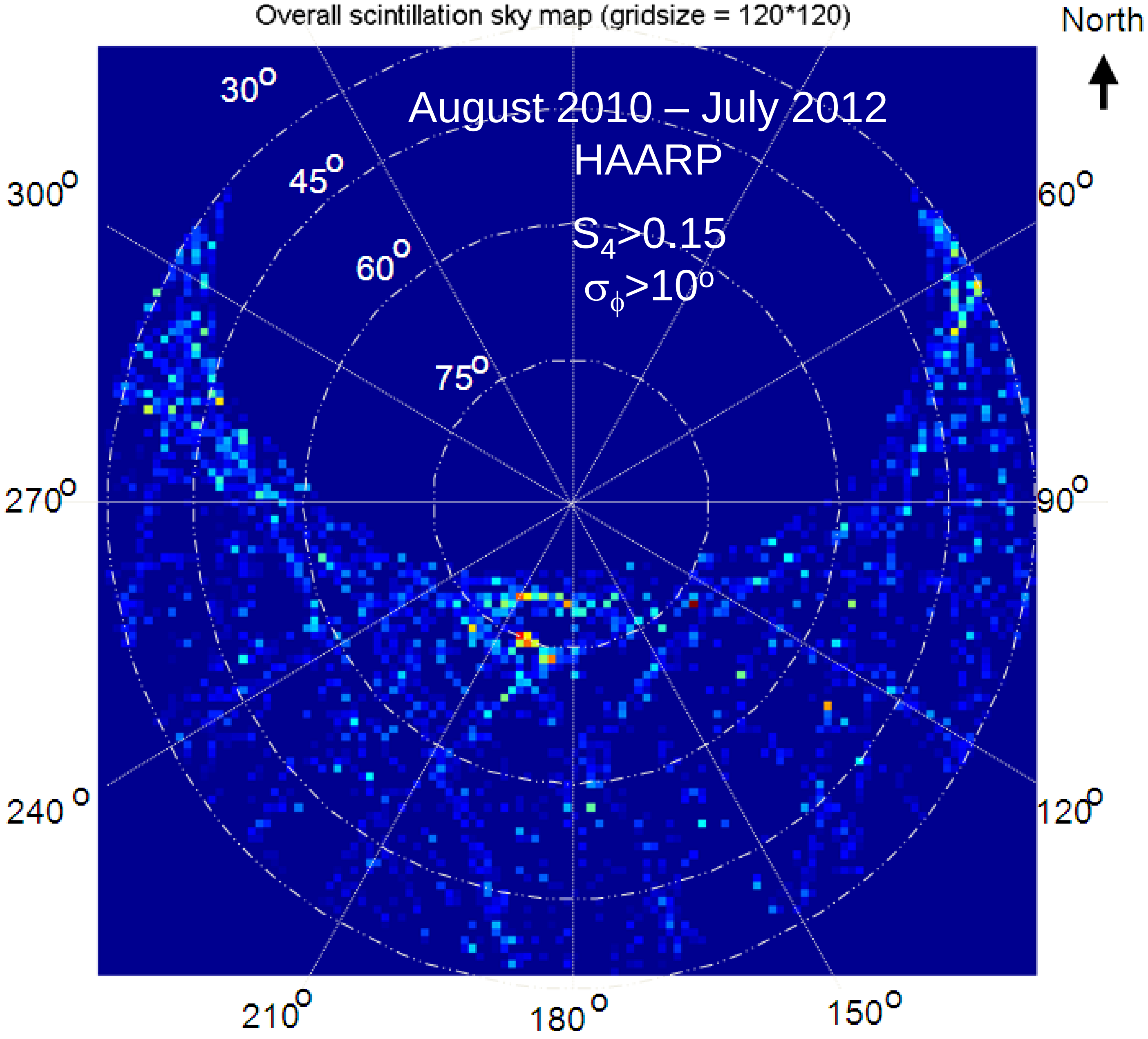

High Latitude Scintillation Temporal Distribution

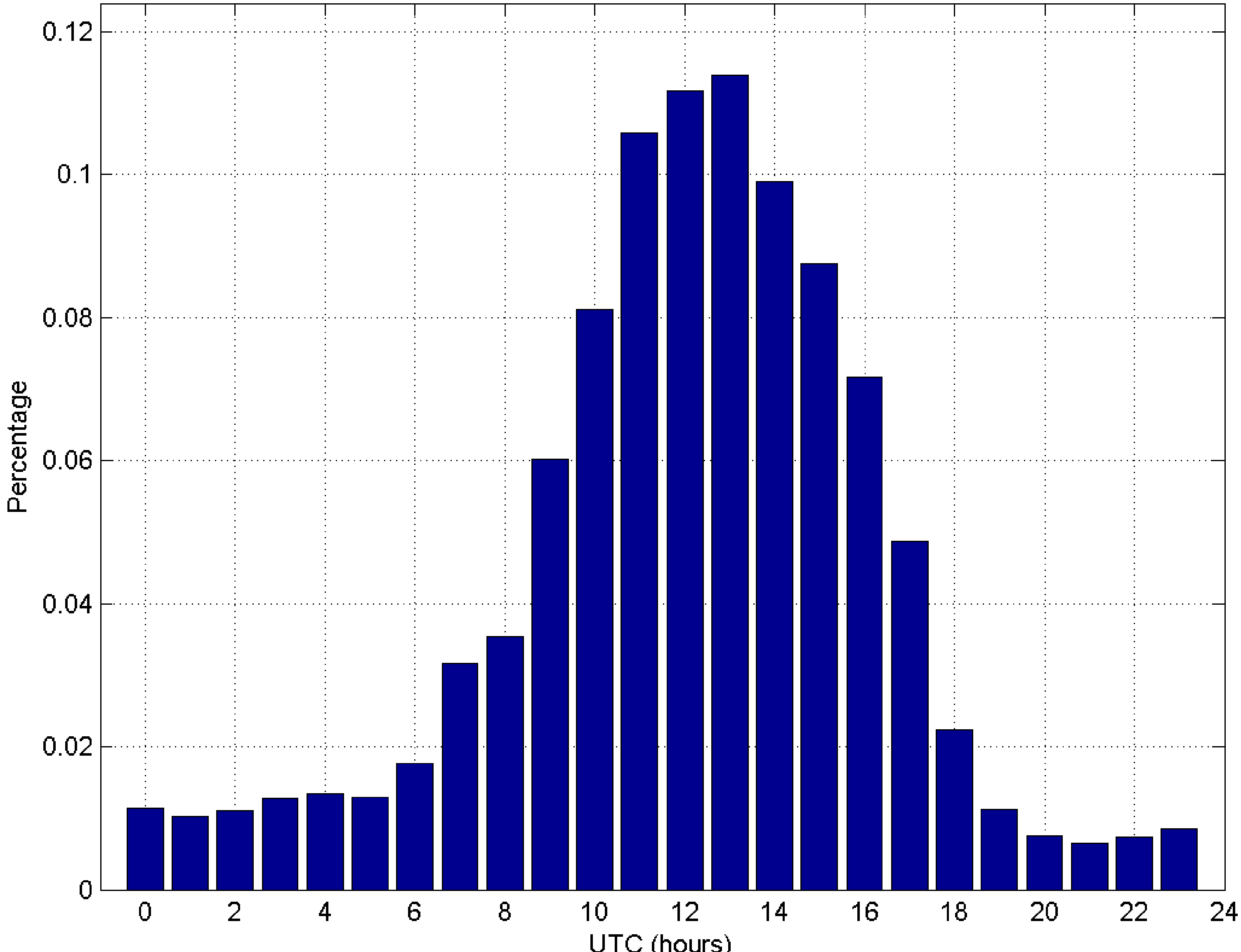

Event Duration Distribution

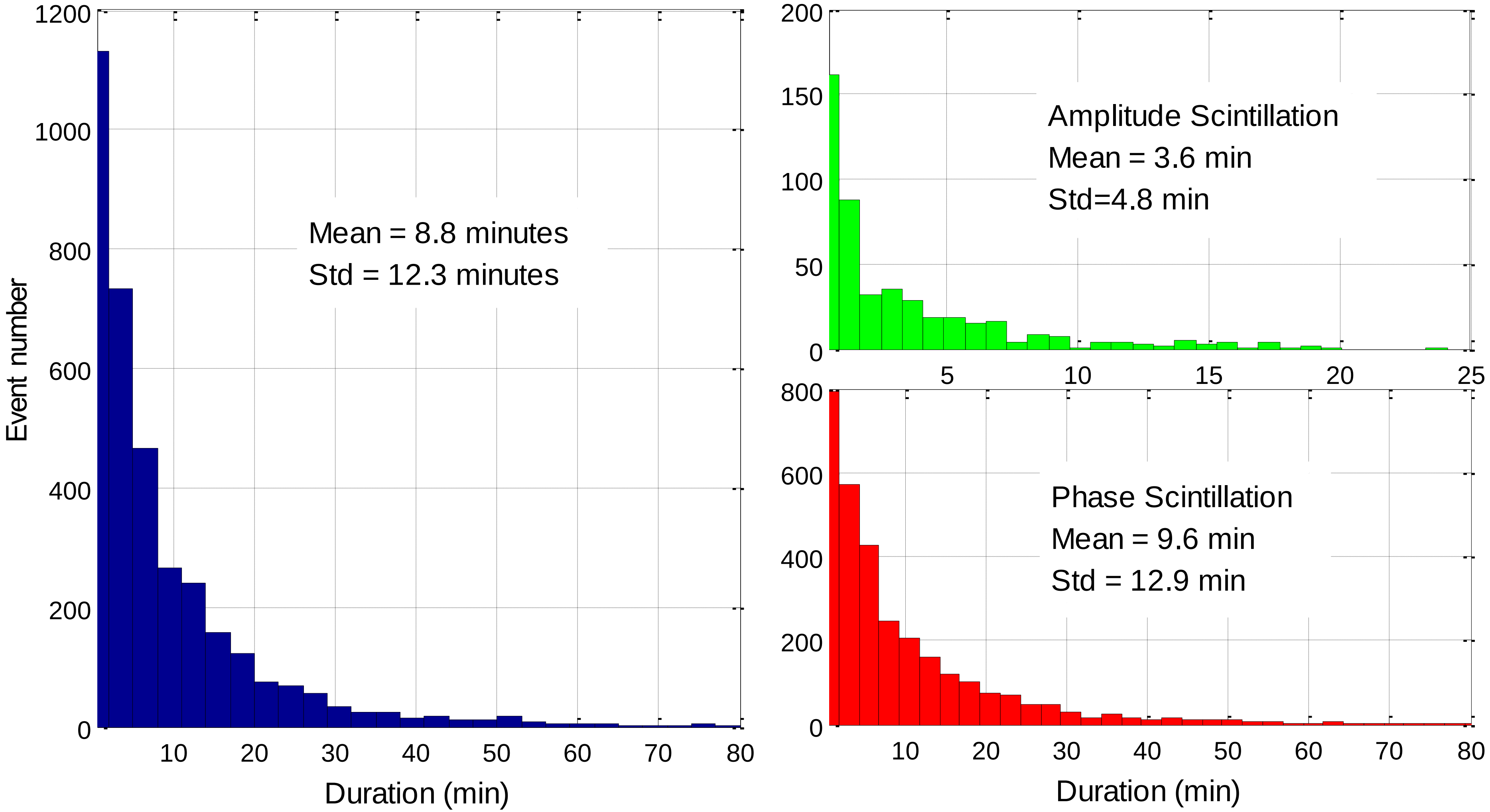

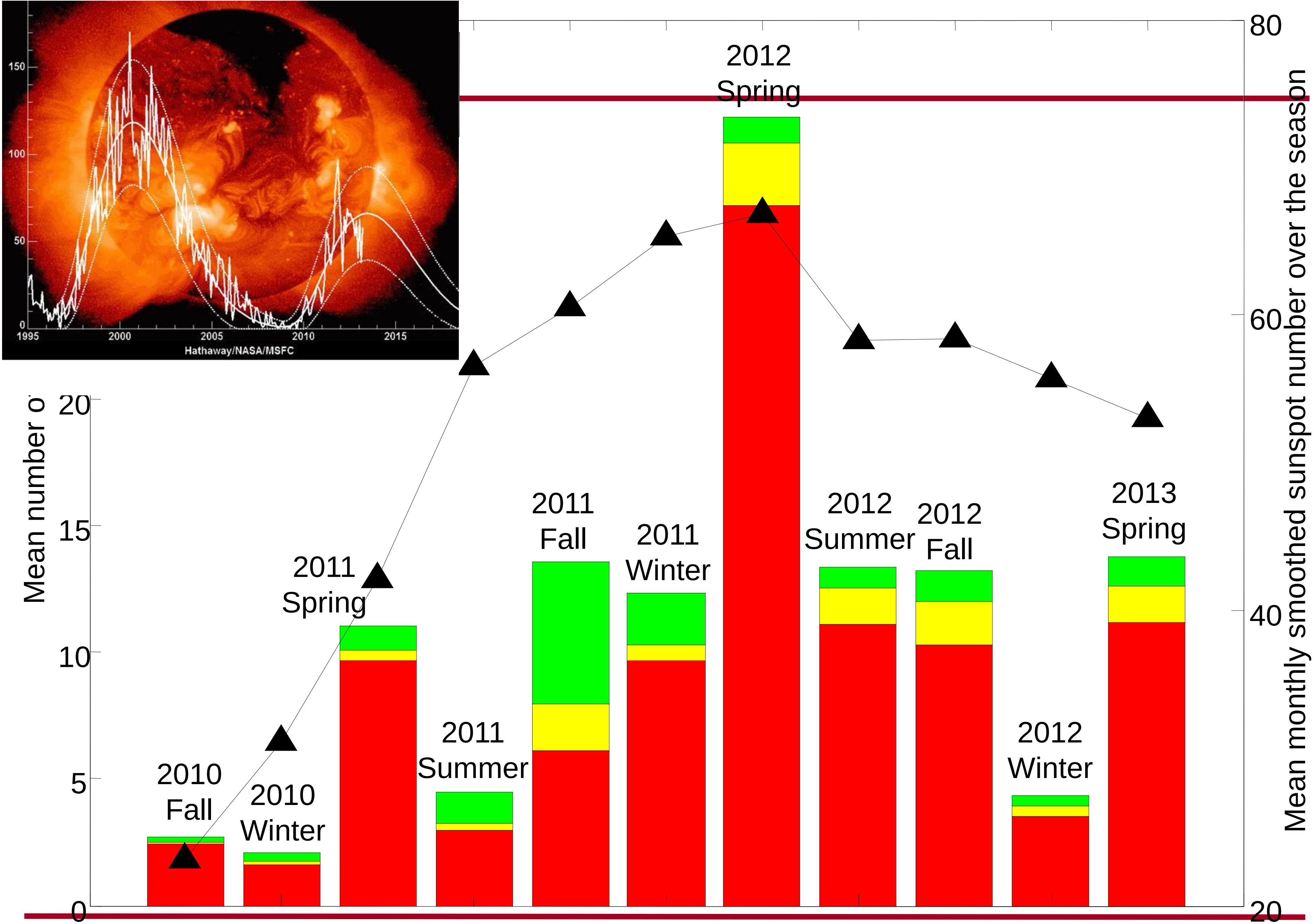
150
100
50
0
1995
2000
2005
2010
2015
Hathaway/NASA/MSFC
Mean number o
0
5
10
15
20
Mean monthly smoothed sunspot number over the season
20
40
60
80
2010 Fall
2010 Winter
2011 Spring
2011 Summer
2011 Fall
2011 Winter
2012 Spring
2012 Summer
2012 Fall
2012 Winter
2013 Spring

Scintillation Impact on PPP

Hong Kong

08/31/2012

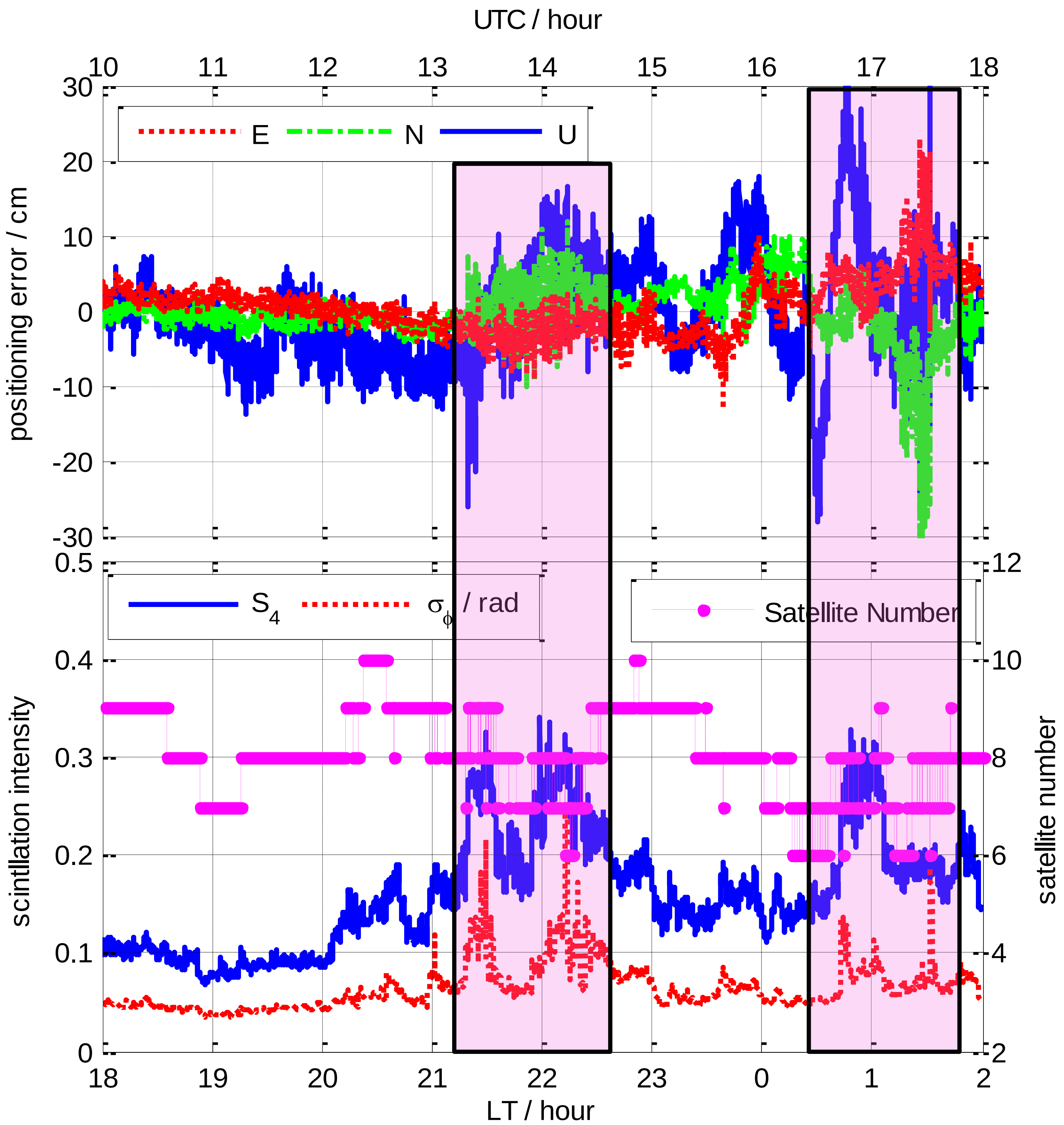

MIAMI UNIVERSITY

Robust Receiver Tracking: Vector Loop vs. Scalar Loop

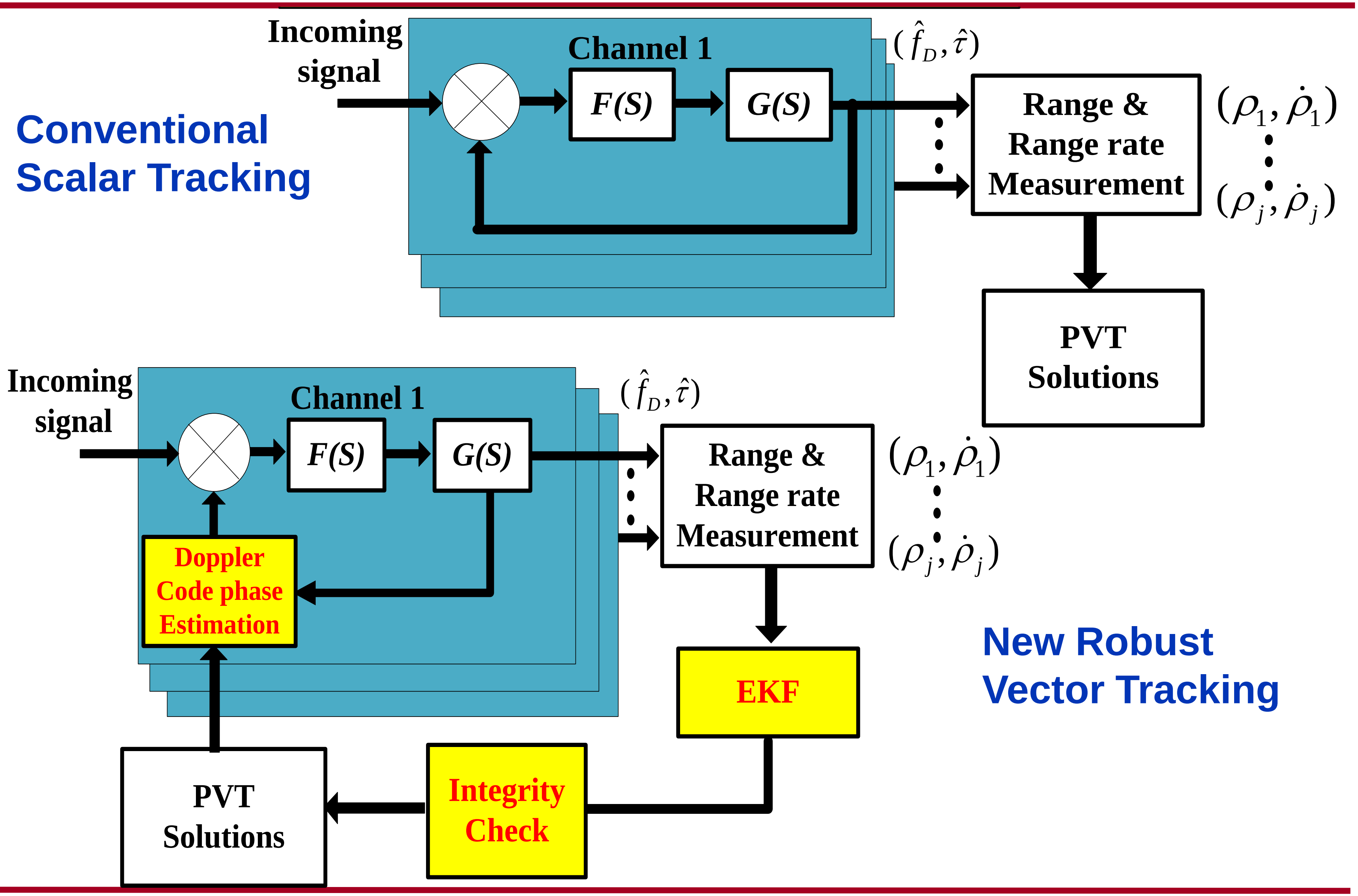

Ascension Island Strong Scintillation Vector Tracking

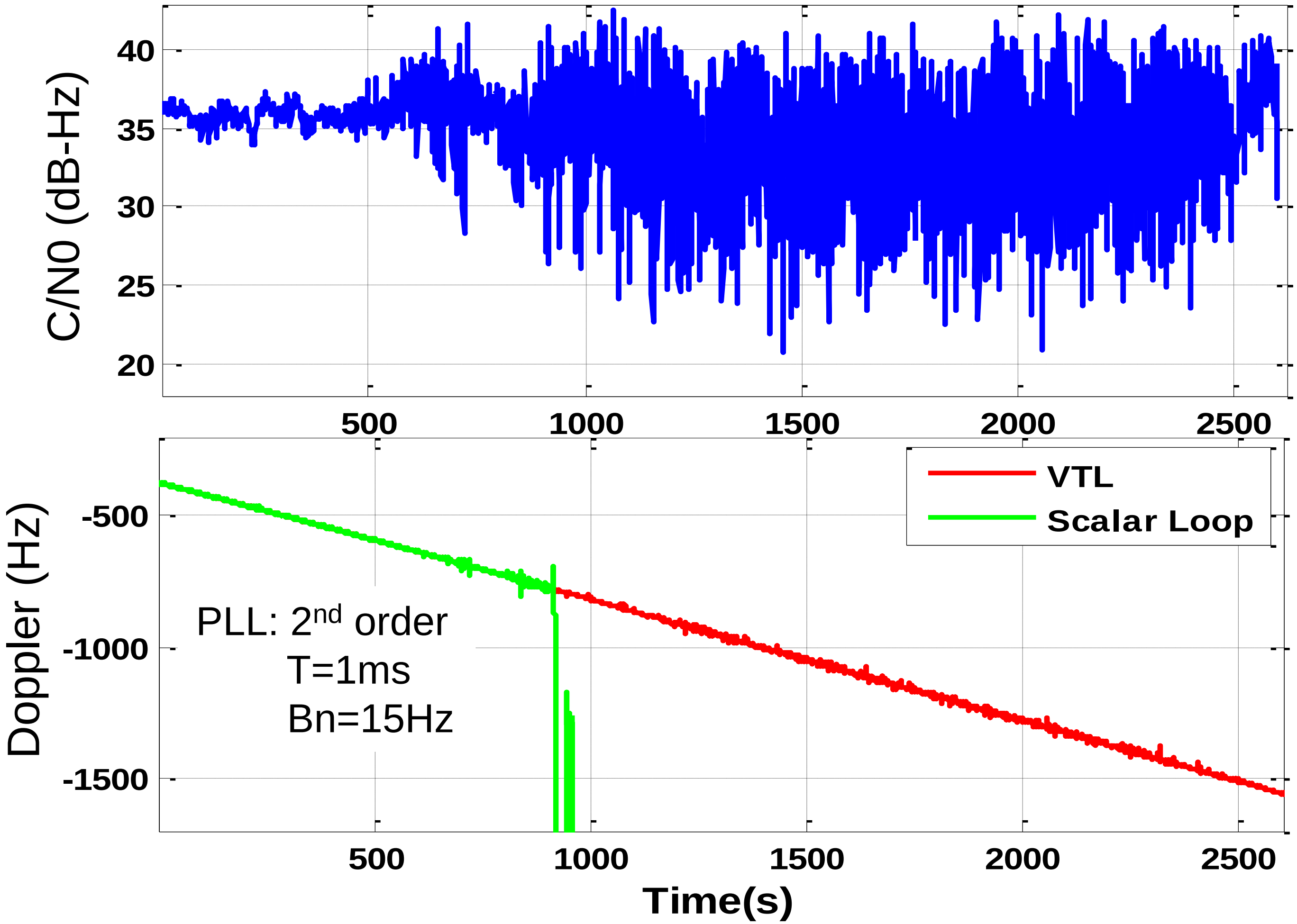

Computation performance is a major challenge!!!

Ionospheric Scintillation On-Going Efforts

- **Deployment enhancement**
- **Data analysis on GLONASS, Galileo, and Compass signals**
- **Multi-frequency scintillation analysis**
- **Accurate signal parameter estimation algorithms**
- **Real time receiver processing**
- **Scintillation tomography**
- **Global scintillation climatology**
- **Joint experimental campaign with other remote sensing instruments**